Biophysical Journal Volume 65 October 1993 1632–1647

Ca^{2+} Transients in Cardiac Myocytes Measured with High and Low Affinity Ca^{2+} Indicators

Joshua R. Berlin and Masato Konishi*
Bockus Research Institute, Graduate Hospital, Philadelphia, Pennsylvania 19146 USA

ABSTRACT Intracellular calcium ion ($[Ca^{2+}]_i$) transients were measured in voltage-clamped rat cardiac myocytes with fura-2 or furaptra to quantitate rapid changes in $[Ca^{2+}]_i$. Patch electrode solutions contained the K^+ salt of fura-2 (50 μM) or furaptra (300 μM). With identical experimental conditions, peak amplitude of stimulated $[Ca^{2+}]_i$ transients in furaptra-loaded myocytes was 4- to 6-fold greater than that in fura-2-loaded cells. To determine the reason for this discrepancy, intracellular fura-2 Ca^{2+} buffering, kinetics of Ca^{2+} binding, and optical properties were examined. Decreasing cellular fura-2 concentration by lowering electrode fura-2 concentration 5-fold, decreased the difference between the amplitudes of $[Ca^{2+}]_i$ transients in fura-2 and furaptra-loaded myocytes by twofold. Thus, fura-2 buffers $[Ca^{2+}]_i$ under these conditions; however, Ca^{2+} buffering is not the only factor that explains the different amplitudes of the $[Ca^{2+}]_i$ transients measured with these indicators. From the temporal comparison of the $[Ca^{2+}]_i$ transients measured with fura-2 and furaptra, the apparent reverse rate constant for Ca^{2+} binding of fura-2 was at least $65 s^{-1}$, much faster than previously reported in skeletal muscle fibers. These binding kinetics do not explain the differences in the size of the $[Ca^{2+}]_i$ transients reported by fura-2 and furaptra. Parameters for fura-2 calibration, R_{min}, R_{max}, and β, were obtained in salt solutions (in vitro) and in myocytes exposed to the Ca^{2+} ionophore, 4-Br A23187, in EGTA-buffered solutions (in situ). Calibration of fura-2 fluorescence signals with these in situ parameters yielded $[Ca^{2+}]_i$ transients whose peak amplitude was 50–100% larger than those calculated with in vitro parameters. Thus, in vitro calibration of fura-2 fluorescence significantly underestimates the amplitude of the $[Ca^{2+}]_i$ transient. These data suggest that the difference in amplitude of $[Ca^{2+}]_i$ transients in fura-2 and furaptra-loaded myocytes is due, in part, to Ca^{2+} buffering by fura-2 and use of in vitro calibration parameters.

INTRODUCTION

Furaptra, the fluorescent indicator sensitive to Mg^{2+} and Ca^{2+}, has been shown to be useful for measuring stimulated $[Ca^{2+}]_i$ transients in rat cardiac myocytes (Cleeman and Morad, 1991; Konishi and Berlin, 1993). A surprising result, however, was that the size of the $[Ca^{2+}]_i$ transients averaged 1.5 μM and were as large as 3–4 μM in some cells (Konishi and Berlin, 1993). Fluorescent Ca^{2+} indicators more commonly used in single myocytes, such as indo-1 and fura-2, report $[Ca^{2+}]_i$ transients which, on average, are only several hundred nanomolar in amplitude (Bers et al., 1990; Cleeman and Morad, 1991). The finding that these indicators report $[Ca^{2+}]_i$ transients of different amplitude may point out our limited ability to quantitate transient changes in $[Ca^{2+}]_i$ and, in general, to measure $[Ca^{2+}]_i$ in cardiac myocytes.

Measurements of $[Ca^{2+}]_i$ in skeletal muscle have also been performed with a wide variety of Ca^{2+} indicators (reviewed by Blinks et al., 1982), and similar to the results above, the apparent amplitude of the $[Ca^{2+}]_i$ transient in response to a stimulus varies quite widely with the Ca^{2+} indicator used (Maylie et al., 1987a, b). Much of this variability has been attributed to differences in the Ca^{2+} affinity (and consequently, the kinetics of Ca^{2+} binding) and the degree of indicator binding to intracellular constituents (Hirota et al., 1989). These two factors may also affect Ca^{2+} measurements in heart muscle, and they suggest that using a variety of Ca^{2+} indicators could be important for determinations of $[Ca^{2+}]_i$ in cardiac myocytes.

Fura-2 has a high affinity for Ca^{2+} with an in vitro K_D close to 200 nM (Grynkiewicz et al., 1985). Given that $[Ca^{2+}]_i$ can exceed this level during the stimulated $[Ca^{2+}]_i$ transient (Allen and Kurihara, 1978; Cannell et al., 1987; Bers et al., 1990; Cleeman and Morad, 1991), a high degree of Ca^{2+} binding to the indicator is expected. Furthermore, high affinity for Ca^{2+} results in ion binding kinetics that limit the ability of these indicators to accurately follow rapid changes in $[Ca^{2+}]_i$. In fact, the Ca^{2+} binding kinetics of fura-2 have been calculated to be much slower in the cellular environment (Baylor and Hollingworth, 1988; Klein et al., 1988) than in salt solutions (Jackson et al., 1987; Kao and Tsien, 1988), so that this problem may be particularly important. Limited binding kinetics and saturation of fura-2 have been shown to lead to underestimates of peak $[Ca^{2+}]_i$ during twitches in skeletal muscle fibers; however, the possibility of similar limitations for fura-2 have not been well studied in cardiac muscle.

An additional concern with the use of high affinity indicators such as fura-2 is that they may significantly contribute to the Ca^{2+} buffering capacity within the cardiac myoplasm (Backx and ter Keurs, 1993). This problem is potentially much greater in cardiac myocytes than skeletal muscle fibers because the smaller capacity of the intrinsic Ca^{2+} buffers and the need to achieve usable signal-to-noise ratios in spite of

Received for publication 22 February 1993 and in final form 13 July 1993.

Address reprint requests to Joshua R. Berlin at the Bockus Research Institute, Graduate Hospital, 415 S. 19th St., Philadelphia, PA 19146.

*Present address: Department of Physiology, Jikei University School of Medicine, 3-25-8 Nishi-shinbashi, Minato-ku, Tokyo 105, Japan.

0006-3495/93/10/1632/16 $2.00

the small size (i.e., short pathlength) of heart cells. Similar considerations would also apply to the use of other high affinity Ca^{2+} indicators, such as indo-1, in cardiac myocytes.

The utility of furaptra as a Ca^{2+} indicator derives from several factors. The structure of furaptra is quite similar to fura-2, with the same chromophore but lacking the nitrobenzyl ring adjacent to the chelation sites (Raju et al., 1989). As a result, the optical properties of furaptra are quite similar to fura-2, so that the same equipment can be used for both indicators. The Ca^{2+} affinity of furaptra (approximately 50 μM; Raju et al., 1989), however, is 250 times lower than fura-2. This lower Ca^{2+} affinity suggests that factors such as saturation, buffering, and kinetics of Ca^{2+} binding are less likely to be major limitations in the ability of furaptra to report rapid and large changes in $[Ca^{2+}]_i$.

Thus, in this study, we have compared $[Ca^{2+}]_i$ transients measured in rat cardiac myocytes with fura-2 and furaptra to investigate whether Ca^{2+} buffering and Ca^{2+} binding kinetics are factors in the measurement of transient changes of $[Ca^{2+}]_i$ in cardiac myocytes. Some of these results have been published previously in abstract form (Konishi and Berlin, 1991; Berlin and Konishi, 1992).

EXPERIMENTAL PROCEDURES

General

The experimental techniques used in this study and the experimental set-up have been described previously (Berlin et al., 1989; Konishi and Berlin, 1993). In brief, enzymatically dispersed single ventricular myocytes of the rat heart were placed in a superfusion bath (Cannell and Lederer, 1986) on the stage of an inverted microscope and superfused with a solution containing (in mM) 140 NaCl, 4 KCl, 1 $MgCl_2$, 2 $CaCl_2$, 10 Glucose, 10 HEPES (*N*-(2-hydroxyethyl)piperizine-*N'*-(2-ethanesulfonic acid)), pH 7.4. Cells were voltage-clamped with a single patch electrode (Hamill et al., 1981) which contained an intracellular salt solution (in millimolar): 70 cesium glutamate, 50 KCl, 15 CsCl, 1 $MgCl_2$, 2.5 ATP, K^+ salt, 0.01 EGTA, and 25 PIPES (1,4-piperazinediethanesulfonic acid, pH 7.2) that included either fura-2 at the indicated concentration or furaptra (300 μM) as a K^+ salt. In experiments shown in Fig. 5 *B*, 10 mM NaCl was added to the electrode solution without adjusting for changes in ionic strength. Zero current and background fluorescence were measured after gigOhm seal formation. The membrane patch under the electrode was then ruptured to establish a whole cell voltage clamp and allow diffusion of the indicator into the cell. Except where indicated, measurements were carried out when indicator loading was near equilibrium. Fluorescence at 500 nm was measured as described in Konishi and Berlin (1993) with illumination wavelengths of 340 and 380 nm for fura-2, and 350 and 370 nm for furaptra.

All data were recorded on videotape (Instrutech, VR-100, Elmont, NY) and digitized off-line at 1 KHz (A2D+; Medical Systems, Greenvale, NY) with an eight-pole Bessel low-pass filter at 500 Hz (−3 dB). Furaptra transients reported here are the average of six to eight fluorescence transients measured at each illumination wavelength. Fura-2 transients are determined from two transients recorded with consecutive depolarizations, one at each illumination wavelength.

Experiments were performed at room temperature (23–24°C).

In vitro calibration

In order to estimate parameter values for fluorescence calibration, in vitro measurements of fura-2 and furaptra fluorescence were carried out on the experimental equipment using glass capillaries approximately 100 μm in diameter. For furaptra, Ca^{2+}-dependent changes in fluorescence were determined using HEDTA (*N*-hydroxyethylenediaminetriacetic acid)-buffered solutions (Konishi and Berlin, 1993). The calculated K_D(Ca) for furaptra was 47 μM and K_D(Mg) was 3.6 mM. For fura-2, calibration solutions contained (in millimolar) 140 KCl, 1 $MgCl_2$, 1 μM fura-2 (K^+ salt), 5 EGTA, and 10 PIPES, pH 7.2. Various amounts of $CaCl_2$ were added to achieve the desired free $[Ca^{2+}]$ according to the computer program, MaxChelator (written by Chris Patton, Hopkins Marine Station) which uses equations from Fabiato and Fabiato (1979) with dissociation constants determined by Harrison and Bers (1987) and Martell and Smith (1974). Fig. 1 shows the relationship between the ratio of fura-2 fluorescence intensity versus $[Ca^{2+}]$. The K_D was calculated to be 239 nM by fitting the raw fluorescence intensity versus log $[Ca^{2+}]$ data with a sigmoid curve which assumed one-to-one binding stoichiometry (not shown).

Calibration of furaptra signals

Calibration of furaptra fluorescence signals was carried out as described previously (Konishi and Berlin, 1993). Briefly, fluorescence intensity at 500 nm was measured during illumination with 350 and 370 nm light. Fluorescence measured during illumination with 350-nm light was taken to be the isosbestic point. Fluorescence during 370-nm illumination was then multiplied by the change in the fluorescence intensity during 350-nm illumination to correct for movement artifacts ($Fl_{corr}(t)$). The change in the Ca^{2+}-sensitive portion of $Fl_{corr}(t)$ was then converted to a fractional change in the free indicator ($\Delta f_D(t)$) by the following:

$$\Delta f_D(t) = \frac{Fl_{corr}(t) - Fl_i}{Fl_{corr}(\text{rest}) - Fl_i} \qquad Fl_i = Fl_{corr}(\text{rest}) \times \frac{\epsilon_b}{\epsilon_f} \tag{1}$$

where Fl_{corr}(rest) is the fluorescence intensity during 370-nm illumination just prior to the voltage clamp depolarization, Fl_i is the Ca^{2+}-insensitive component of the fluorescence signal during 370-nm illumination, and ϵ_f and ϵ_b are the fluorescence coefficients for Ca^{2+}-free and -bound forms of the indicator, respectively. The value of ϵ_b/ϵ_f was 0.1 from in vitro calibrations as described by Konishi and Berlin (1993). To determine if this value might be significantly altered by indicator binding to proteins in the

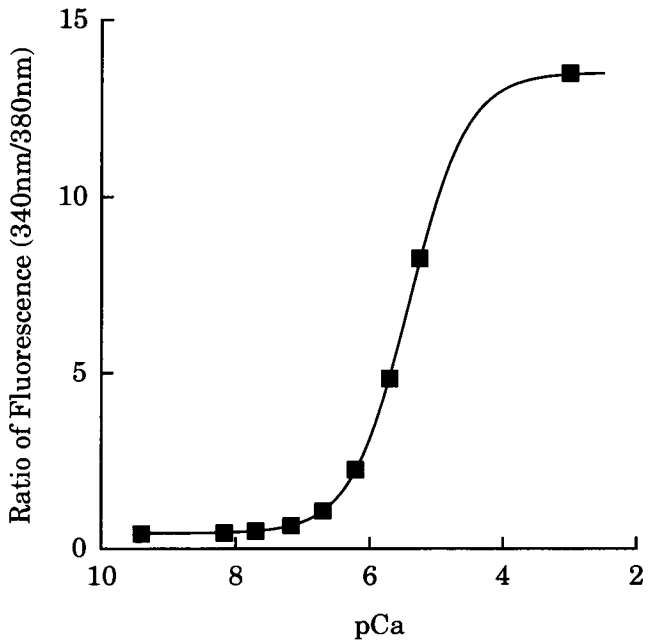

FIGURE 1 In vitro calibration of fura-2. Calibration of fura-2 in a 100-μm diameter glass capillary. The solid line was determined by fitting the data with a nonlinear least squares routine to a sigmoid equation with the following parameters: R_{min} = 0.43, R_{max} = 13.4, and $K_D \cdot \beta$ = 3.2 μM, Hill coefficient = 1.

cell, calibrations were also carried out in the presence of 20 mg/ml Aldolase, a protein concentration that appears to bind most of the furaptra. Under these conditions, ϵ_b/ϵ_f averaged 0.12 in two trials. The value of ϵ_b/ϵ_f determined in the absence of Aldolase was used to convert furaptra fluorescence to $[Ca^{2+}]_i$.

The apparent K_D for Ca^{2+} is much higher than the $[Ca^{2+}]_i$ concentrations encountered in these studies. Thus, $\Delta f_D(t)$ converts directly to $\Delta[Ca^{2+}]_i$, as in the following:

$$\Delta[Ca^{2+}]_i = K_D \times [1 - \Delta f_D(t)] = K_D \times \Delta f_{DCa}(t) \quad (2)$$

where $\Delta f_{DCa}(t)$ is the change in the fraction of Ca^{2+}-bound indicator and K_D is calculated to be 54 μM in Konishi and Berlin (1993) and in the present study. This calibration procedure assumes that $[Mg^{2+}]_i$ is 0.5 mM and that it does not change significantly during the $[Ca^{2+}]_i$ transient. These assumptions were addressed in Konishi and Berlin (1993).

Calibration of fura-2 signals

Fura-2 fluorescence signals from cells were calibrated in terms of $[Ca^{2+}]_i$ with the ratiometric calibration procedure used by Grynkiewicz et al. (1985).

$$[Ca^{2+}] = K_D \times \beta \times \frac{(R - R_{min})}{(R_{max} - R)} \quad (3)$$

where R_{min}, R_{max}, and β have their usual meaning. For the most calibrations, values of 0.45, 14.6, and 13.1 obtained in vitro (see above) were used for R_{min}, R_{max}, and β, respectively (in vitro calibration).

In some cells, in situ estimation of these parameter values for fura-2 fluorescence was performed by a modification of the method of Li et al. (1987). At the end of an experiment, the myocyte was superfused for 15 min with an EGTA-buffered, Ca-ionophore solution containing (in millimolar) 140 NaCl, 4 KCl, 2 $MgCl_2$, 10 glucose, 2.5 K_2EGTA, 0.025 4-Br A23187, 0.01 nigericin, 0.010 "1799" (bis-(hexafluoracetonyl)acetone) and 10 HEPES, pH 7.4 (R_{min} solution). Cell fluorescence was monitored periodically until fluorescence ratio reached a new steady-state. The superfusion solution was then changed to a high Ca^{2+} solution containing (in millimolar) 145 KCl, 1 $MgCl_2$, 2 $CaCl_2$, 10 glucose, 10 HEPES, pH 7.4 (R_{max} solution). After several minutes, during which time the fluorescence ratio reached a maximum, the superfusion solution was changed to a Mn^{2+} solution containing (in millimolar) 140 NaCl, 4KCl, 1 $MgCl_2$, 1 $MnCl_2$, 10 glucose, 10 HEPES, pH 7.4 (R_{back} solution) to determine the level of background fluorescence.

The R_{min} solution contained the compound 1799, a nonfluorescent mitochondrial uncoupler. Control experiments demonstrated that background fluorescence (reflecting the cellular NAD/NADH balance) changed on exposure to 1799, but remained unchanged thereafter. Thus, to calculate fura-2-dependent fluorescence, fluorescence values obtained in R_{back} were subtracted from those values obtained in R_{min} solution and R_{max} solution. For calculation of fura-2 fluorescence levels prior to exposure to 1799, background fluorescence determined after seal formation (at the beginning of the experiment) was subtracted from total cell fluorescence (Berlin et al., 1989).

Estimation of intracellular fura-2 concentration

In some experiments, cytosolic fura-2 concentration in myocytes was estimated by comparing fluorescence levels in cells and in glass capillaries filled with a fura-2 containing solution (see below).

Myocytes were voltage-clamped with electrodes containing an intracellular salt solution with 50 μM fura-2. After establishing a whole-cell voltage clamp, fluorescence levels were allowed to come to a steady state (approximately 15 min). Fluorescence intensity was measured during illumination with 360-nm light, and the illumination area was limited to approximately 50–75 μm by a field stop in the illumination path. The cell was positioned so that both ends of the cell were beyond the edge of the illumination field. The isosbestic point for the indicator was chosen for these experiments so that fluorescence levels would be Ca^{2+}-independent. Konishi et al. (1988) found that fluorescence intensity of fura-2 is affected by protein binding; however, no corrections for changes in indicator fluorescence properties were performed.

In these experiments, cells with simple geometry were chosen to facilitate determination of cell dimensions. Cell width was measured using a reticle in the eyepiece. Cell depth was measured by determining the distance between the first in-focus plane at the top and bottom surfaces of the cell viewed with a CCD camera. Focusing depth was calibrated using latex beads with diameters of 5–25 μm. Intracellular volume accessible to fura-2 was calculated assuming the cell was a rectangular parallelepiped with 25% of cell volume occupied by membrane-bound structures (e.g., mitochondria) which excluded the indicator. After determination of the intracellular volume accessible to fura-2, fluorescence intensity was normalized to accessible volume.

Immediately following the determination of cell fluorescence, glass capillaries with diameters between 10 and 20 μm (similar to cell depth) were placed under the microscope without changing the illumination field stop. The capillaries were filled with the same intracellular solution used in the voltage-clamping electrodes. Fluorescence levels were measured during 360-nm illumination, and background fluorescence was measured in capillaries filled with indicator-free solutions. Inside diameters were measured using the eyepiece reticle so that the volume of illuminated solution could be calculated. Fluorescence was also normalized to illuminated volume.

Cytosolic fura-2 concentration was then calculated as the ratio of normalized fluorescence intensities of the cell and the capillary multiplied by 50 μM.

Materials

All chemicals were reagent grade. furaptra (Magfura-2, tetrapotassium salt, lot 9A), fura-2 (pentapotassium salt), BAPTA (tetrapotassium salt), 4-Br A23187, and nigericin were purchased from Molecular Probes Inc. (Eugene, OR). Compound 1799 was a generous gift of Du Pont Inc. (Wilmington, DE).

Statistics

Statistical values are expressed as mean ± SE. Statistical significance was tested by two-tailed t tests ($p < 0.05$).

RESULTS

Fig. 2 shows a typical $[Ca^{2+}]_i$ transient elicited with depolarizations of 50-ms duration from −70 to +10 mV delivered at 0.2 Hz. The myocyte was voltage-clamped with an electrode containing 50 μM fura-2. The middle panel shows the ratio of fluorescence intensities calculated after subtraction of background fluorescence at the two illumination wavelengths (340 and 380 nm). The change in fluorescence ratio was then converted to $[Ca^{2+}]$ using a calibration curve similar to that in Fig. 1 with the assumption that Ca^{2+} was in rapid equilibrium with fura-2. Using this in vitro calibration method, resting $[Ca^{2+}]_i$ in the myocyte was estimated to be 39 nM and the peak of the $[Ca^{2+}]_i$ transient, estimated to be 422 nM, was reached 32 ms after the beginning of the depolarization. $[Ca^{2+}]_i$ declined thereafter but, even after 500 ms, remained slightly elevated. The time course of this transient is typical for those experiments carried out at room temperature. Table 1 shows that the average amplitude of the $[Ca^{2+}]_i$ transient was 395 ± 63 nM and the time to peak $[Ca^{2+}]_i$ was estimated at 39 ± 2 ms.

These experiments were performed under identical experimental conditions as experiments in which the Ca^{2+} indicator was furaptra (Konishi and Berlin, 1993). The results of experiments using furaptra are also summarized in Table 1.

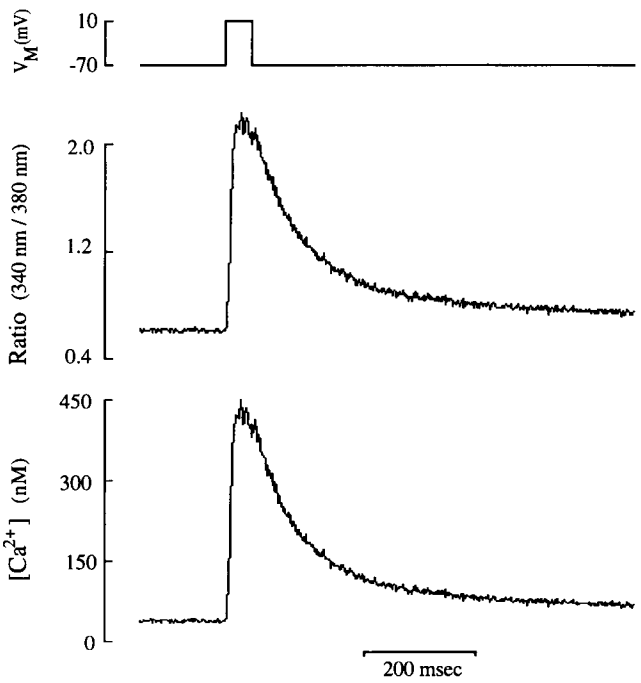

FIGURE 2 $[Ca^{2+}]_i$ transient measured with fura-2. The voltage (top), ratio of 500-nm fluorescence intensities (middle), and $[Ca^{2+}]_i$ transient (bottom) are shown for a myocyte voltage clamped with an electrode containing 50 μM fura-2. The calibration parameters for conversion of ratio to $[Ca^{2+}]_i$ are R_{min} = 0.41, R_{max} = 13.0, β = 13.1, and K_D = 239 nM.

TABLE 1 Calcium transients measured with fura-2 and furaptra

	fura-2	furaptra
	Mean ± SE	
$[Ca^{2+}]$ (nM)		
Rest	48 ± 7	
Peak	440 ± 48	1523 ± 252
ISO effect (% increase)	41 ± 12	84 ± 24
Time-to-peak (ms)	39 ± 1	36 ± 3
Calculated peak $[Ca^{2+}]_{tot}$ (μM)	58 ± 8	77 ± 9

Summary data of $[Ca^{2+}]_i$ transients measured in cells (n = 5–7) voltage-clamped with electrodes containing 50 μM fura-2 or 300 μM furaptra. Data for furaptra loaded cells from Konishi and Berlin (1993).

As previously described (Konishi and Berlin, 1993), furaptra signals allow changes in $[Ca^{2+}]_i$, but not resting $[Ca^{2+}]_i$, to be determined. Thus, the obvious difference between $[Ca^{2+}]_i$ transients reported with fura-2 and furaptra, is that the average amplitude of the $[Ca^{2+}]_i$ transients measured with furaptra are almost four times larger than those measured with fura-2. In spite of the difference in amplitude, the average time-to-peak $[Ca^{2+}]_i$ was similar. These results suggest that a major discrepancy exists between $[Ca^{2+}]_i$ transients determined in myocytes loaded with fura-2 and those cells loaded with furaptra. In order to resolve the apparent discrepancy in the size of the $[Ca^{2+}]_i$ transients reported by these two indicators, several possibilities were explored.

A potential problem with the comparison made in Table 1 was that the accumulated data were obtained from experiments performed on different experimental days. Since significant day-to-day variability is observed with acutely dissociated myocytes, it is difficult to rule out the possibility that the difference in peak amplitude (and the similarity in time to peak) is fortuitous. In order to overcome this day-to-day variability, a series of experiments were performed on the same day in which cells were divided into two groups where the Ca^{2+} indicator was fura-2 or furaptra. It was necessary to perform experiments in different cells, because the optical properties of fura-2 and furaptra are almost identical. The amplitude of $[Ca^{2+}]_i$ transients calibrated from furaptra and fura-2 fluorescence signals were 1.98 ± 0.23 μM (n = 4) and 0.31 ± 0.10 μM (n = 3), respectively. The time to peak $[Ca^{2+}]_i$ was, on the other hand, 29 ± 3 ms (n = 4) and 42 ± 8 ms (n = 3) for furaptra and fura-2 transients, respectively (see Fig. 5 *B* and below). Thus, the results from the same day also demonstrate that $[Ca^{2+}]_i$ transients from fura-2-loaded cells are significantly smaller ($p < 0.05$ by t test) in peak amplitude (by a factor of 6.4).

One explanation for this result was that fura-2 underestimated the true $[Ca^{2+}]_i$ during the transient, because it became highly saturated. To test this possibility we examined the effect of 10 μM isoproterenol on the size of the $[Ca^{2+}]_i$ transient in fura-2-loaded cells. As expected, exposure to isoproterenol increased the peak amplitude of the $[Ca^{2+}]_i$ transient (41%, on average). The magnitude of this effect was smaller but not significantly different than the increase in the $[Ca^{2+}]_i$ transient observed in furaptra-loaded myocytes (Table 1). Thus, although fura-2 becomes more highly bound with Ca^{2+} than furaptra, the level of fura-2 binding remains below saturation.

Other possible explanations for the discrepancy in the amplitude of $[Ca^{2+}]_i$ transients reported by fura-2 and furaptra could include 1) Ca^{2+} buffering by fura-2, 2) slow Ca^{2+} binding kinetics of fura-2, and 3) errors in calibration of the fluorescence signals. All three of these potential factors are examined below.

Fura-2 buffering of $[Ca^{2+}]_i$

Differences in the size of the $[Ca^{2+}]_i$ transient measured with furaptra and fura-2 may reflect significant buffering of the $[Ca^{2+}]_i$ transient by fura-2. This explanation is plausible, because the Ca^{2+} affinity of fura-2 (K_D = 239 nM under in vitro conditions) is near physiological $[Ca^{2+}]_i$ so that it could greatly increase the Ca^{2+} buffering capacity of the cell. This possibility was tested by measuring the stimulated fluorescence transient at various times during indicator loading from a voltage clamp electrode containing 50 μM fura-2 (Fig. 3). The top panels show the fura-2 fluorescence level increased threefold during measurements made 120, 320, and 570 s after establishing a whole-cell voltage clamp. However, during indicator loading, it is clear that the size of the $[Ca^{2+}]_i$ transient, estimated as fluorescence ratio, is decreased several-fold. These data are shown as fluorescence ratio rather than $[Ca^{2+}]_i$ to demonstrate that simple calibration errors arising from changes in signal-to-noise ratio, as

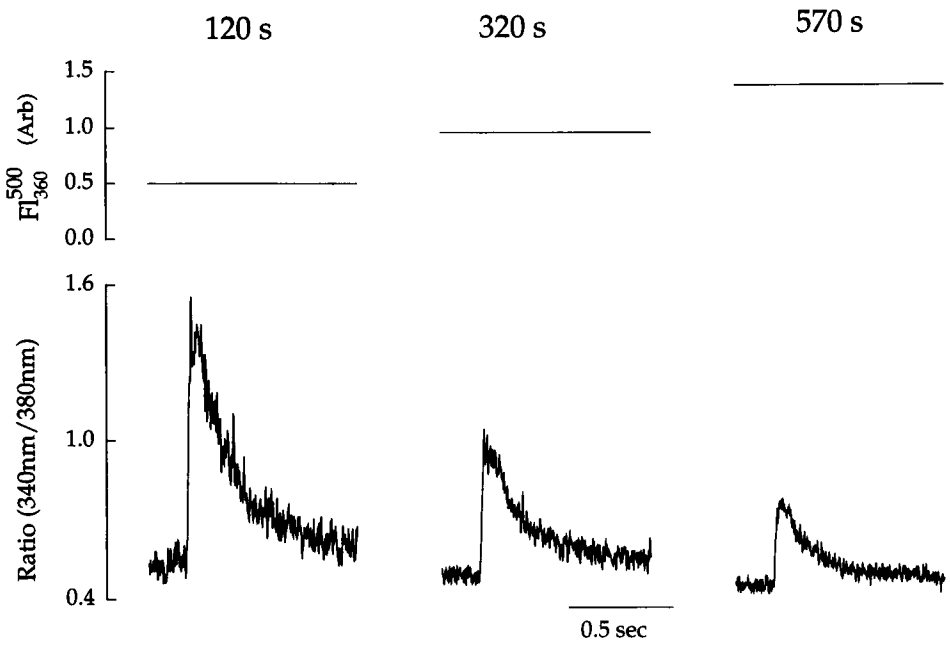

FIGURE 3 Effect of fura-2 loading on the amplitude of the $[Ca^{2+}]_i$ transient. The top panels show the level of fluorescence measured at the isosbestic point, with 360-nm illumination. The time after establishing a whole cell voltage clamp is indicated. The bottom panels show the $[Ca^{2+}]_i$ transient, displayed as the ratio of fluorescence intensity, elicited by 50 ms depolarizations from −70 to +10 mV.

the indicator loads, do not explain the decrease in the size of the $[Ca^{2+}]_i$ transient.

This result is at odds with the effect of indicator loading reported by Cleeman and Morad (1991) where an 8-fold change in fura-2 concentration (up to 400 μM) was reported to have little effect on the peak of the $[Ca^{2+}]_i$ transient. One reason for these contradictory results could be that cell dialysis in the present experiments causes a time-dependent decrease in the size of the $[Ca^{2+}]_i$ transient, independent of changes of cellular fura-2 concentration. Because fura-2 loading was not reversed in these experiments, it is not possible to exclude this possibility. However, consistent with this idea, the amplitude of the inward current elicited by a depolarizing voltage clamp pulse did decrease 40% during the period of fura-2 loading (data not shown). Thus, we can not rule out that factors other than fura-2 concentration affect the size of the $[Ca^{2+}]_i$ transient.

To avoid the problems inherent in the experiment above, the effects of fura-2 on Ca^{2+} buffering were estimated in another set of experiments in which the size of the $[Ca^{2+}]_i$ transient was compared in furaptra-loaded cells and cells loaded with low concentrations of fura-2 (10 μM in the voltage clamp electrode). To minimize the variability inherent in comparing $[Ca^{2+}]_i$ transients in different cells, experiments in fura-2 and furaptra-loaded myocytes were performed on the same days. Fig. 4 shows the average $[Ca^{2+}]_i$ transient determined in four fura-2-loaded (*left panel*) and six furaptra-loaded myocytes (*right panel*). In both sets of experiments, $[Ca^{2+}]_i$ transients were elicited by 50-ms depolarizations from −70 to +10 mV delivered every 5 s. The average peak $[Ca^{2+}]_i$ and the maximal change in $[Ca^{2+}]_i$ during the transient in the fura-2-loaded myocytes was calibrated to be 438 ± 76 and 387 ± 65 nM, respectively. In contrast, the average peak change in $[Ca^{2+}]_i$ in the furaptra loaded myocytes was calibrated to be 821 ± 202 nM. The ratio of peak $[Ca^{2+}]_i$ change reported by furaptra and fura-2 was 2.1; however, the difference was not statistically significant. This result contrasts with experiments using 5-fold higher concentrations of fura-2 where this ratio was 3.9 (Table 1) or 6.4 (above) and the amplitude of transients measured with furaptra were significantly larger than those measured with fura-2. Together these results suggest that Ca^{2+} buffering explains, at least in part, the difference in the size of the $[Ca^{2+}]_i$ transients reported by the two indicators.

It is worth noting that the average size of the $[Ca^{2+}]_i$ transients measured with fura-2 in Table 1 and Fig. 4 are very similar despite the 5-fold differences in fura-2 concentration in the voltage clamp electrode. Although, the cellular concentrations of fura-2 were not quantitated in these two sets of experiments, it was nonetheless very clear that the intracellular fura-2 concentration was greatly reduced when the pipette concentration of fura-2 was reduced. This conclusion is based upon the observation that the level of fura-2 fluorescence was much less in cells loaded with the indicator from pipettes containing 10 μM fura-2 as compared to those voltage clamped with pipettes containing 50 μM fura-2. Thus, our a priori assumption was that the $[Ca^{2+}]_i$ transient measured in cells loaded with a lower concentration of fura-2 should be larger. In fact, as the ratio of furaptra transients to fura-2 transients points out, the relative size of the fura-2 transient is larger. The similarity in the absolute amplitude of the transients simply reflects the smaller $[Ca^{2+}]_i$ transients in this series of experiments. This is most clearly seen by comparing the $[Ca^{2+}]_i$ transients measured with furaptra. The average amplitude of the transients was only half of that reported in Table 1 despite the fact that both sets of experiments were carried out under identical experimental conditions and with equal pipette indicator concentrations. These results, however, do point out the variability inherent in working with acutely dissociated myocytes and demonstrate

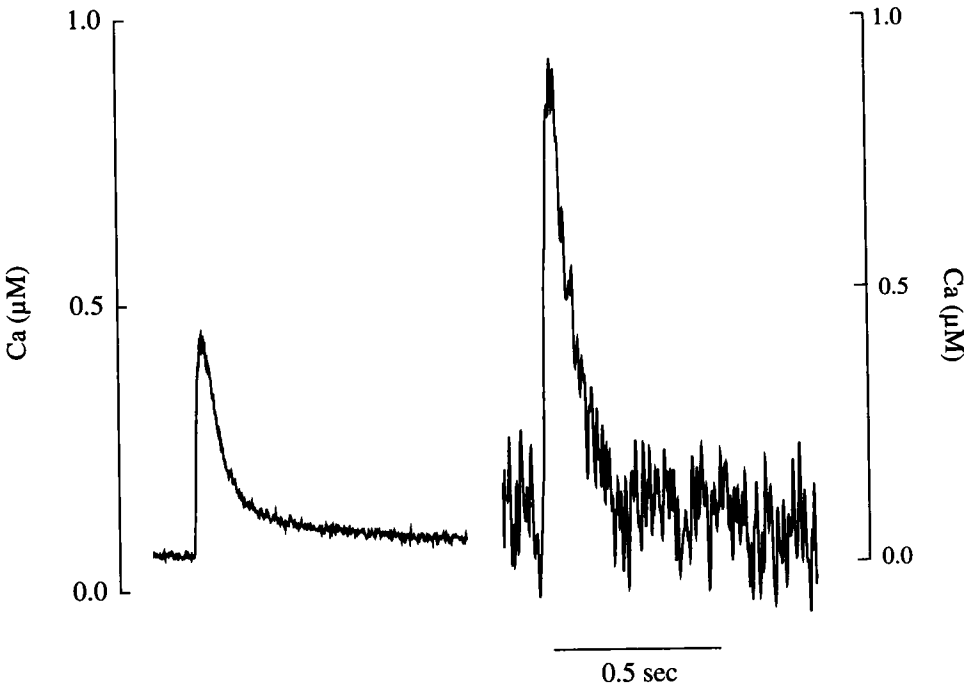

FIGURE 4 Comparison of $[Ca^{2+}]_i$ transients in cells loaded with low fura-2 concentrations and furaptra. $[Ca^{2+}]_i$ transients were elicited by 50-ms depolarizations from −70 to +10 mV. The electrode solution contained 10 μM fura-2 (left panel) or 300 μM furaptra (right panel). The $[Ca^{2+}]_i$ transients displayed are the average of $[Ca^{2+}]_i$ transients observed in four cells loaded with fura-2 and six cells loaded with furaptra.

the importance of doing experiments on the same set of cells, as was done here, when trying to draw comparisons between different experimental maneuvers.

The experiments shown in Figs. 3 and 4 demonstrate that increasing cellular fura-2 concentrations buffer the $[Ca^{2+}]_i$ transient. However, optical and Ca^{2+} binding properties of fura-2 have been shown to change in the cellular environment (Li et al., 1987; Konishi et al., 1988), and it is possible that these changes are dependent on the cellular concentration of the indicator.

To ensure that the apparent buffering of $[Ca^{2+}]_i$ by fura-2 was not an experimental artifact arising from changes in indicator optical properties, furaptra fluorescence transients were measured in the presence and absence of the nonfluorescent, high affinity Ca^{2+} buffer, BAPTA. In these experiments, myocytes were voltage-clamped with electrodes containing 300 μM furaptra and depolarized at 0.2 Hz from −70 to +10 mV for 100 ms. In three cells, the peak change in $[Ca^{2+}]_i$ during the transient was 854 ± 110 nM. When 100 μM BAPTA was also included in the pipette solution for four cells, the peak change in $[Ca^{2+}]_i$ was significantly reduced to 221 ± 58 nM ($p < 0.05$). Thus, increasing the buffering capacity of the pipette solution decreased the amplitude of the $[Ca^{2+}]_i$ transient, consistent with the ability of fura-2 to buffer the $[Ca^{2+}]_i$ transient.

Kinetics of Ca^{2+} binding to fura-2

Because fura-2 has high affinity for binding with Ca^{2+}, there has been concern about the ability of this indicator to accurately follow rapid changes in $[Ca^{2+}]$. Klein et al. (1988) and Baylor and Hollingworth (1988) have examined the kinetics of Ca^{2+} binding to fura-2 in skeletal muscle fibers. Both investigations found that the forward and reverse rate constants for Ca^{2+} complexation were much slower in myoplasm than rate constants determined in free solution (Jackson et al., 1987; Kao and Tsien, 1988). The slow reverse rate constant, in particular, estimated in skeletal muscle raises the possibility that fura-2 might not follow the most rapid changes in $[Ca^{2+}]_i$ during the cardiac muscle $[Ca^{2+}]_i$ transient so that the estimate of peak $[Ca^{2+}]_i$ might be erronously small.

The Ca^{2+} affinity of furaptra is more than 200 times less than fura-2. If the forward rate constant for Ca^{2+} complexation is diffusion limited (approximately 1×10^8 M^{-1} s^{-1} in myoplasm; Baylor and Hollingworth, 1988), the difference in their apparent affinities would lie in their reverse rate constants. It is, then, likely that furaptra can accurately report more rapid changes in $[Ca^{2+}]$. In fact, furaptra's fluorescence change appeared to track fast $[Ca^{2+}]_i$ transients in frog skeletal muscle with little kinetic delay (Konishi et al., 1991). Thus, by comparing the fluorescence transients recorded with furaptra and fura-2, it may be possible to determine whether fura-2 fluorescence signals lag behind the true changes in $[Ca^{2+}]_i$.

Fig. 5 *A* compares the $[Ca^{2+}]_i$ transients measured in cells loaded with furaptra and a low concentration of fura-2 (10 μM in the pipette). For temporal comparison, the average $[Ca^{2+}]_i$ transient of four fura-2-loaded cells is scaled (2.1 times) to the same amplitude as the average $[Ca^{2+}]_i$ transient of six furaptra-loaded cells. The time-to-peak $[Ca^{2+}]_i$ of the average fura-2 transient is not significantly delayed with respect to the furaptra transient. These data show that the Ca^{2+} binding kinetics of fura-2 do not lead to significant alterations in the waveform of the

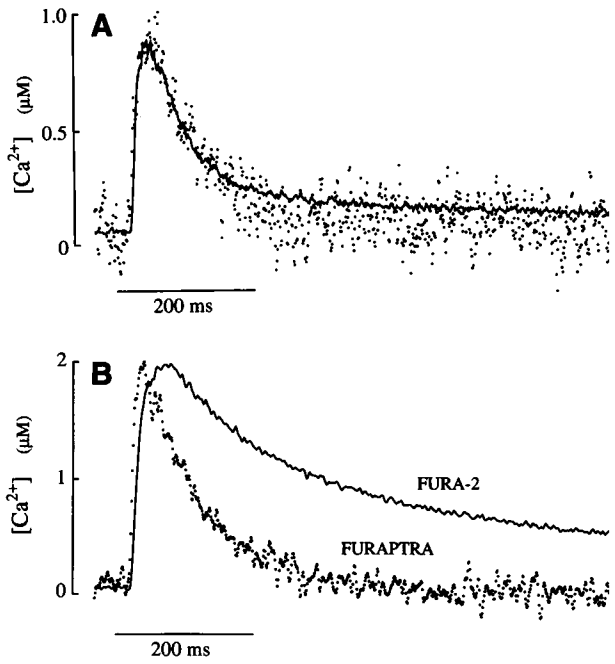

FIGURE 5 Comparison of the time course of $[Ca^{2+}]_i$ transients measured with furaptra (*dots*) and two fura-2 (*solid lines*) concentrations. $[Ca^{2+}]_i$ transients were elicited by 50-ms depolarizations from −70 to +10 mV. Cells were loaded with furaptra by voltage-clamping with pipettes containing 300 μM indicator. (*A*) The average $[Ca^{2+}]_i$ transient in cells loaded with low fura-2 concentration (10 μM in the pipette) is scaled by a factor of 2.1 to match the peak of furaptra $[Ca^{2+}]_i$ transient and superimposed on the average transient in furaptra-loaded cells (same data as Fig. 4). (*B*) Average $[Ca^{2+}]_i$ transients calculated from three cells loaded with fura-2 (50 μM in the pipette) and four cells loaded with furaptra. The average $[Ca^{2+}]_i$ transient of the fura-2-loaded cells is scaled by a factor of 6.4 to match the peak for the average transient in furaptra-loaded cells.

observed $[Ca^{2+}]_i$. Thus, fura-2 kinetics in the myocyte appear to be fast enough to measure peak $[Ca^{2+}]_i$.

Fig. 5 *B* shows a similar comparison in cells loaded with furaptra or a higher concentration of fura-2 (50 μM in the pipette). As in Fig. 5 *A*, experiments were carried out on the same day in myocytes loaded with fura-2 and furaptra to minimize the effects of day-to-day variability. Interestingly, the time to peak $[Ca^{2+}]_i$ of the average transient measured with fura-2 is clearly delayed with respect to the transient measured with furaptra (47 vs. 29 ms) and the rate of decline of the transient is slower. A similar slowing of the $[Ca^{2+}]_i$ transient was observed in two cells voltage-clamped with pipettes containing 100 μM fura-2. Since fura-2 appears to significantly buffer Ca^{2+} during the transient (see above and Appendix I), this delay could reflect the alteration of cellular $[Ca^{2+}]_i$-dependent Ca^{2+}-handling processes (for example, Ca^{2+} release from the sarcoplasmic reticulum; see Discussion) or errors in calculation of the $[Ca^{2+}]_i$ transient from changes in furaptra fluorescence (Konishi and Berlin, 1993; see Discussion).

Calibration of fura-2

Another possible reason for the discrepancy between the size of the $[Ca^{2+}]_i$ transients reported by fura-2 and furaptra could be an artifact arising from the different calibration procedures used to convert fluorescence to $[Ca^{2+}]_i$ (Konishi and Berlin, 1993). In Figs. 2–5, the data have been converted from fluorescence to $[Ca^{2+}]$ using calibration parameters that were determined on the experimental apparatus using isotonic salt solutions. Several reports, however, demonstrate that these parameters are likely to be different for indicators in salt solutions and in the intracellular melieu (Li et al., 1987; Konishi et al., 1988; Hove-Madsen and Bers, 1992).

In the present study, the effects of changes in three of these parameters, R_{min}, R_{max}, and β, were examined to determine their importance in affecting the conversion of fura-2 fluorescence to $[Ca^{2+}]_i$. Experiments were performed so that R_{min}, R_{max}, and β were determined in fura-2-loaded cells by a method similar to that of Li et al. (1987). Briefly, at the end of an experiment, the superfusion solution was changed from the normal HEPES-buffered Tyrode's solution to a Ca^{2+}-free Tyrode's solution which contained 2.5 mM K_2EGTA, the Ca^{2+}-ionophore, 4-Br A23187, the K^+/H^+ antiporter, nigericin, and the mitochondrial uncoupler, 1799. The purpose of this solution was to inhibit normal cellular Ca^{2+} metabolism and decrease $[Ca^{2+}]_i$ to very low levels. Indicator fluorescence was followed until it reached a new steady state, usually 15 min, and R_{min} was determined. The superfusion solution was then changed to a Na^+-free (K^+ substituted), 2 mM Ca^{2+}-containing solution to estimate R_{max}. After several minutes in this solution, a 1 mM $MnCl_2$-containing Tyrode's solution was introduced to determine the level of background fluorescence. In several cells, this solution change protocol resulted in a marked decrease in cell fura-2 concentration as judged by a large wavelength-independent decrease in fluorescence intensity. These cells were excluded from analysis of R_{max} and β. In other cells, indicator levels did not appear to markedly change during the calibration procedure. Some leakage of the indicator may still have occurred. However, only β would tend to be overestimated in this case while R_{min} and R_{max} would not be affected.

The values of R_{min}, R_{max} and β for fura-2 determined in vitro with salt solutions were, respectively, 0.45 ± 0.03, 14.60 ± 1.6 (n = 3), and 13.1 (determined in a glass capillary), whereas the corresponding values of 0.35 ± 0.03 (n = 11), 6.1 ± 0.4 (n = 5), and 9.6 ± 0.9 (n = 5) were obtained in fura-2-loaded myocytes. All three parameters were decreased when determined in myocytes as compared to salt solutions. Of particular note, is the large decrease in R_{max} which was less than half the value in salt solutions. It is possible that this low value resulted from dialysis of the low $[Ca^{2+}]$ pipette solution against the cell interior. This seems unlikely because, after exposure to "1799," the cells underwent an irreversible contracture which was accompanied by a very large increase of input resistance into the cell. This suggested that cell dialysis was minimal. Furthermore, in one cell where the voltage clamp electrode was removed prior to the calibration procedure, the value of R_{max} was similar to the other in situ calibration trials. Thus, in myocytes, the Ca^{2+}-dependent optical properties of fura-2 are

different than in salt solutions, consistent with the results of Li et al. (1987).

Fig. 6 shows the effect of using R_{min}, R_{max}, and β determined in the cell on the conversion of fluorescence data to $[Ca^{2+}]_i$. The myocyte was held at −70 mV and $[Ca^{2+}]_i$ transients were elicited with the same voltage clamp protocol used in Fig. 2. The top panel shows the ratio of fluorescence intensities and the bottom panel shows superimposed transients which have been converted to $[Ca^{2+}]_i$. The smaller transient was calculated with parameters determined in vitro as in Fig. 1, while the larger transient was calculated with R_{min}, R_{max}, and β determined in this myocyte. There is little change in the value of resting $[Ca^{2+}]_i$, because R_{min} determined in this cell was very close to the in vitro value (0.39 vs. 0.41, respectively). On the other hand, the peak $[Ca^{2+}]_i$ was calculated to be 350 nM with the parameters determined in the myocyte vs. 191 nM with in vitro parameters. This difference is due to the value of R_{max} which was 7.3 in this cell (versus 13.1 from an in vitro calibration). Thus, using calibration parameters determined in the cell, the size of the $[Ca^{2+}]_i$ transient was calculated to be 83% larger than when using in vitro parameters.

If these in situ calibration parameters were applied to the data in Fig. 4 in which low concentrations of fura-2 were used, resting and peak $[Ca^{2+}]_i$ during the transients were 158 ± 24 nM and 953 ± 195 nM (n = 4), respectively. The peak change in $[Ca^{2+}]_i$, 795 ± 175, was not significantly different than the change of $[Ca^{2+}]_i$ in furaptra-loaded myocytes, 821 ± 202 nM (n = 6). Thus, by accounting for the effects of Ca^{2+} buffering by fura-2 and the changes in optical properties of the indicator in the cell, the $[Ca^{2+}]_i$ transients reported by fura-2 and furaptra appear to be similar.

The other calibration parameter, K_D, was not determined in the myocyte. Binding to cellular proteins, in particular, may decrease the Ca^{2+} affinity of these indicators (Konishi et al., 1988). In preliminary experiments, shifts in K_D for Ca^{2+} were observed for fura-2 and furaptra in the presence of aldolase and albumin (Mapp and Berlin, unpublished data). It is not clear, however, that these shifts in K_D reflect the change in K_D in the cell (Backx and ter Keurs, 1993) because the magnitude of the affinity shift may be dependent on protein concentration and possibly the protein species (Konishi et al., 1988; Uto et al., 1991). Furthermore, attempts to measure K_D in the cell were not successful.

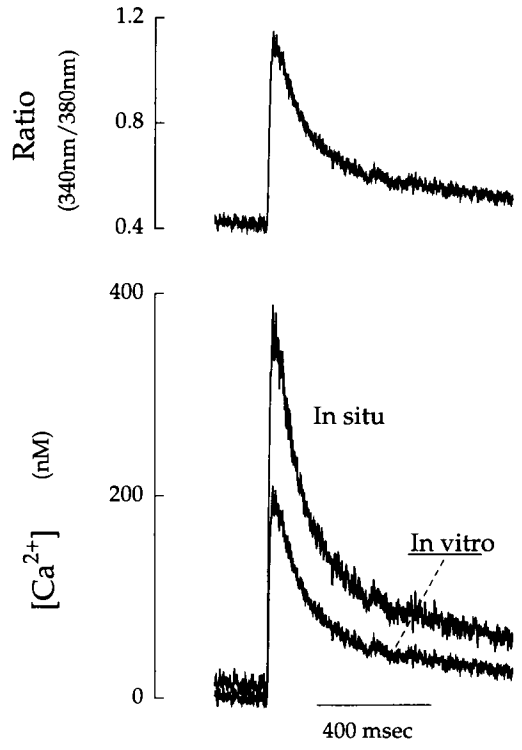

FIGURE 6 In vitro and in situ calibration of fura-2 fluorescence. The top panel shows the ratio of fluorescence intensities signal for a fura-2-loaded myocyte. The cell was depolarized from −70 to +10 mV for 50 ms. The bottom panel shows superimposed $[Ca^{2+}]_i$ transients calculated by converting the fluorescence ratio signal to $[Ca^{2+}]_i$ with calibration parameters determined in salt solutions (in vitro) or in the cell at the end of the experiment (in situ) with the Ca^{2+} ionophore, 4-Br A23187 (see Methods). Calibration parameters: K_D = 239 nM; in vitro: R_{min} = 0.42, R_{max} = 13.4, β = 13.1; in situ: R_{min} = 0.39, R_{max} = 7.2, β = 9.8.

DISCUSSION

The purpose of this study was to re-examine the utility of using fura-2 to measure transient changes of $[Ca^{2+}]_i$ in cardiac myocytes. Fura-2 and indo-1 are widely used to measure transient changes of $[Ca^{2+}]_i$ in cardiac cells, and a major advantage of these indicators is thought to be the relative ease with which $[Ca^{2+}]_i$ can be quantitated. There are, however, many reports suggesting that the ability to quantitate $[Ca^{2+}]_i$ with these indicators may be complicated by a number of factors including changes in the Ca^{2+}-dependent optical properties in the cell interior (Li et al., 1987), changes in ion affinity due to protein binding (Konishi et al., 1988) and solution viscosity (Roe et al., 1990), and indicator quenching by heavy metals (Roe et al., 1990). Surprisingly, other potential issues, such as Ca^{2+} buffering and dye saturation, which also affect the $[Ca^{2+}]_i$ reported by these indicators have not been investigated in cardiac cells.

One obvious way to check the measurements of Ca^{2+} made with fura-2 (or indo-1) is to have indicators with different Ca^{2+} binding properties. An obvious candidate for such a Ca^{2+} indicator is the bioluminescent protein, aequorin. The Ca^{2+} binding stoichiometry of aequorin, however, is quite complex and, furthermore, measuring $[Ca^{2+}]_i$ in single cells has proved to be technically challenging (Cobbold and Bourne, 1984).

Recently, Konishi et al. (1991) demonstrated that the indicator, furaptra, originally reported as a Mg^{2+} indicator (Raju et al., 1989), could also be used to measure transient changes of $[Ca^{2+}]_i$ in skeletal muscle fibers. Preliminary experiments (Cleeman and Morad, 1991) showed that furaptra could also measure $[Ca^{2+}]_i$ and our previous investigations (Konishi and Berlin, 1993) demonstrated the utility of furaptra as a Ca^{2+} indicator in cardiac myocytes. Furaptra has specific advantages as an indicator to check fura-2. 1) The K_D for Ca^{2+} of furaptra is at least 100-fold less than that of

fura-2. The low affinity minimizes the possibility that furaptra will become saturated within the range of physiological $[Ca^{2+}]_i$ and suggests that the kinetics of Ca^{2+} binding are likely to be much faster than fura-2. 2) The similarity between the structures of fura-2 and furaptra make it more likely that these indicators would interact with intracellular structures in a similar manner. For example, protein binding might have qualitatively similar effects on the two indicators. These considerations suggest that it would be interesting to compare $[Ca^{2+}]_i$ transients measured with furaptra and fura-2 to examine several of the potential complicating factors in the use of fura-2 listed above.

Comparison of $[Ca^{2+}]_i$ transients measured with fura-2 and furaptra

Fig. 2 shows a typical $[Ca^{2+}]_i$ transient and Table 1 shows average data that indicate the amplitude of $[Ca^{2+}]_i$ transients calculated in cells loaded with furaptra was four times larger than the amplitude of $[Ca^{2+}]_i$ transients calculated from fura-2 fluorescence transients. The experimental conditions were identical in all other respects except that cells were loaded with fura-2 (50 μM in the electrode) or furaptra (300 μM in the electrode). In all cases, changes in fluorescence were converted to $[Ca^{2+}]_i$ using parameters (K_D and ϵ_b/ϵ_f for furaptra; K_D, R_{min}, R_{max}, and β for fura-2) determined with in vitro calibration solutions. These data could call into question the accuracy of the $[Ca^{2+}]_i$ transients reported by these indicators. Reasons for this apparent discrepancy are considered below.

One explanation could be that one or both of the indicators have pharmacologic actions in the cell that alter the excitation-contraction coupling mechanism. In fact, we cannot rule out this possibility. However, simple evaluations of the excitation-contraction coupling mechanism can be made in the presence of these indicators. Konishi and Berlin (1992) demonstrated that several experimental maneuvers including exposure to isoproterenol, increasing intracellular Na^+, and increasing voltage clamp pulse duration, all increased the size of the $[Ca^{2+}]_i$ transient measured with furaptra. Similar maneuvers in fura-2-loaded myocytes yielded qualitatively similar effects on the $[Ca^{2+}]_i$ transient (Table 1 and Berlin and Konishi, unpublished observations). Thus, to a first approximation, excitation-contraction coupling behaves in a similar fashion whether the cells are loaded with fura-2 or furaptra.

Konishi and Berlin (1993) also considered the possibility that furaptra does not accurately report peak changes in $[Ca^{2+}]_i$ during the transient. Changes in $[Mg^{2+}]_i$ during the $[Ca^{2+}]_i$ transient could complicate the calibration of Ca^{2+}-dependent changes in furaptra fluorescence and so lead to an overestimate of the amplitude of the $[Ca^{2+}]_i$ transient. A computer simulation that estimates changes in $[Mg^{2+}]_i$ during the $[Ca^{2+}]_i$ transient, however, suggests this error is likely to be very small for the determination of peak changes in $[Ca^{2+}]_i$. Thus, furaptra can be used to estimate the peak of the $[Ca^{2+}]_i$ transient.

It is more likely that the discrepancy lies in the measurement and calibration of $[Ca^{2+}]_i$ with fura-2. One obvious explanation is that fura-2 underestimates $[Ca^{2+}]_i$ at the peak of the transient due to the high degree of Ca^{2+} binding (Marban et al., 1990). Without knowing the K_D of fura-2 in the cell, this possibility can not be excluded. If the K_D in the cell is the same as in vitro calibrations (239 nM), fura-2 is 65% bound with Ca^{2+} at the peak of the average $[Ca^{2+}]_i$ transient. The degree to which fura-2 is likely to underestimate the amplitude of the $[Ca^{2+}]_i$ transient will depend on the size of the spatial gradients of $[Ca^{2+}]_i$ which may exist during rapid release of Ca^{2+} from the sarcoplasmic reticulum (Cannell and Allen, 1984; Wier and Yue, 1986). Our own model (see Appendix II), however, predicts that, even in the extreme, the underestimate would be too small to account for the differences in the amplitude of the $[Ca^{2+}]_i$ transients reported by fura-2 and furaptra.

We also examined three additional factors which could lead fura-2 to underestimate the size of the $[Ca^{2+}]_i$ transient. The results of this study suggest that binding kinetics of Ca^{2+} to the indicators do not explain the discrepancy. On the other hand, buffering of $[Ca^{2+}]_i$ by fura-2 and the determination of calibration parameters do appear to explain, at least in part, the differences in the amplitude of the $[Ca^{2+}]_i$ transients reported by these two indicators.

Buffering of $[Ca^{2+}]_i$ by fura-2

Experimental data and computer simulations (see Appendix I) support the contention that fura-2 significantly buffers $[Ca^{2+}]_i$ during the transient. The intrinsic calcium buffering capacity of myocytes is likely to be in the hundreds of micromolar. However, by comparing the presumed affinity of these intracellular buffers (Fabiato, 1983), it is clear that fura-2 could be potent buffer within the cell, even if the affinity is lower in the cell than in in vitro solutions (Konishi et al., 1988).

Several studies have demonstrated that fura-2 can buffer $[Ca^{2+}]_i$ during stimulated transients. Baylor and Hollingworth (1988) demonstrated that fura-2 concentrations greater than 100 μM caused briefer antipyrylazo III transients, presumably due to buffering of $[Ca^{2+}]_i$ by fura-2. Timmerman and Ashley (1986) showed that fura-2 concentrations as low as 6 μM could buffer the $[Ca^{2+}]_i$ transient in barnacle muscle fibers. The present study also suggests that fura-2 significantly buffers $[Ca^{2+}]_i$. With 50 μM fura-2 in the pipette, the size of the $[Ca^{2+}]_i$ transients were four to six times smaller than those estimated in furaptra-loaded cells under the same experimental conditions. Lowering pipette fura-2 concentration to 10 μM (and also decreasing cellular indicator concentration), decreased the relative difference in the $[Ca^{2+}]_i$ transients measured with fura-2 and furaptra to two to one. These results are further supported by experiments in which the amplitude of $[Ca^{2+}]_i$ transients measured with furaptra were decreased 4-fold with 100 μM BAPTA added to the pipette solution. BAPTA is structurally related to fura-2 and has a similar Ca^{2+} affinity. These experiments demonstrate

it also has similar effects on the $[Ca^{2+}]_i$ transient. Thus, in the range of concentrations used in these experiments, fura-2 does buffer $[Ca^{2+}]_i$ in myocytes.

Backx and ter Keurs (1993) also found that the size of the $[Ca^{2+}]_i$ transient and contractile force decreased as fura-2 concentration increased in iontophoretically injected papillary muscles. However, the change in the size of the $[Ca^{2+}]_i$ transient was much smaller than reported here. The difference may be due to a smaller change in cellular fura-2 concentration or the fact that measurements were made over a 3-h period as fura-2 concentration in the muscle slowly decreased.

Cleeman and Morad (1991) reported that an 8-fold increase in cellular fura-2 concentration (up to 400 μM is presumed by the authors) did not reduce the peak of the stimulated $[Ca^{2+}]_i$. The difference in the present results might be that Cleeman and Morad (1991) also included cAMP in their pipette solution. Thus, as fura-2 loaded in the cell, cAMP also loaded into the cell, so that the level of sarcoplasmic reticulum $[Ca^{2+}]_i$ release would be expected to increase and offset the increased buffering capacity due to fura-2. In contrast, we generally observed a time-dependent decrease in the size of the $[Ca^{2+}]_i$ transient during loading. However, time-dependent changes in excitation-contraction coupling in dialyzed myocytes can not be ruled out unless indicator loading can be reversed. For this reason, experiments such as that shown in Fig. 3 are probably unreliable to judge the ability of fura-2 to buffer $[Ca^{2+}]_i$. This was the motivating reason for conducting the experiments in Fig. 4 at the time when dye loading was near steady state levels. This insured that differing degrees of cell dialysis would not complicate the comparison of $[Ca^{2+}]_i$ transients in fura-2- and furaptra-loaded myocytes.

The ability of fura-2 to buffer $[Ca^{2+}]_i$ during the transient demonstrates that this is one factor which explains the smaller amplitude of $[Ca^{2+}]_i$ transients measured in fura-2 loaded myocytes. The data also point out that Ca^{2+} buffering may not be the only explanation for these differences.

Kinetics of Ca^{2+} binding to fura-2

In frog skeletal muscle fibers, fura-2 does not accurately track fast $[Ca^{2+}]_i$ transients (Baylor and Hollingworth, 1988; Klein et al., 1988). From the fura-2 fluorescence signals in myoplasm, the apparent dissociation rate constant of fura-2 was calculated to be 12 s^{-1} at 6–10°C (Klein et al., 1988) and 23 s^{-1} at 16°C (Baylor and Hollingworth, 1988). These values are substantially smaller than the dissociation constant for fura-2 measured using rapid mixing (84 s^{-1}; Jackson et al., 1987) or temperature-jump apparatus (97 s^{-1}; Kao and Tsien, 1988) in free solution at 20°C. Baylor and Hollingworth (1988) suggested that the slowing of fura-2 binding kinetics in the myoplasm might correlate to the degree of fura-2 binding to intracellular constituents. Thus, it was somewhat of a surprise that the fura-2 $[Ca^{2+}]_i$ transient did not substantially lag behind furaptra $[Ca^{2+}]_i$ transient in cardiac myocytes at 23°C.

The extent of fura-2 binding in the myoplasm appears to be similar in skeletal muscle fibers (Konishi et al., 1988) and cardiac myocytes (Blatter and Wier, 1990). Thus, our a priori expectation was that fura-2 Ca^{2+} binding kinetics would also be similar; however, this does not appear to be the case. A dissociation rate constant of 23 s^{-1} or less would show a significant kinetic lag in the $[Ca^{2+}]_i$ transient signals. In Fig. 5 *A*, no significant kinetic delay is observed. Even in Fig. 5 *B*, where the peak of the $[Ca^{2+}]_i$ transient in fura-loaded cells is delayed with respect to the peak of furaptra $[Ca^{2+}]_i$ transient, the binding kinetics of fura-2 must be much faster than those reported in skeletal muscle (see Appendix II).

One explanation for the more rapid kinetics is that fura-2 binds to different proteins in cardiac cells and skeletal muscle fibers with the consequence that the Ca^{2+} binding properties are altered differently in these two tissues. Konishi et al. (1988) and Uto et al. (1991) have demonstrated that protein binding can alter the K_D of fura-2 for Ca^{2+} (but see Backx and ter Keurs, 1993). Nonetheless, with the exception of parvalbumin (Inaguma et al., 1991), the intracellular proteins in cardiac muscle are more notable for their similarities, rather than their differences, to proteins in skeletal muscle. Since the degree of indicator binding is similar in skeletal (Konishi et al., 1988) and cardiac muscle (Blatter and Wier, 1990), it seems unlikely that differences in indicator protein-binding underlie the apparently faster kinetics of fura-2 observed in cardiac muscle.

Another possibility is that fura-2 Ca^{2+} binding kinetics in skeletal muscle have been underestimated. This explanation takes into account the more rapid rate of Ca^{2+} release from sarcoplasmic reticulum in skeletal muscle and the manner in which fura-2 binding kinetics have been determined (Baylor and Hollingworth, 1988; Klein et al., 1988). The $[Ca^{2+}]_i$ transient measured with furaptra has a much faster time course in skeletal muscle (time to peak 5–6 ms with action potential stimulation at 16°C (Konishi et al., 1991)) than in cardiac muscle (time to peak 30–40 ms at 23°C; this study). Thus, fura-2 fluorescence signals may follow the slower rise of the $[Ca^{2+}]_i$ transient in cardiac muscle with smaller kinetic delay than that expected for the faster $[Ca^{2+}]_i$ transient in skeletal muscle. In addition, the rapid rate of Ca^{2+} release from skeletal muscle sarcoplasmic reticulum (SR) would transiently form a large spatial gradient of $[Ca^{2+}]_i$ (Cannell and Allen, 1984). In the presence of spatial gradients of $[Ca^{2+}]_i$ that lead to a high fraction of the indicator being bound with Ca^{2+}, it is likely that the binding kinetics of fura-2 would be underestimated, because changes in the indicator signal will not only be limited by binding kinetics but also by saturation (see Appendix III).

How important is indicator saturation in affecting the calculation of Ca^{2+} binding kinetics in cardiac and skeletal muscle fibers? This question cannot be answered in absolute terms, but it is likely to be more important in skeletal muscle, where the rate of Ca^{2+} release from SR appears to be more rapid than in cardiac muscle. Furthermore, the peak $[Ca^{2+}]_i$ during the transient is higher (see Baylor and Hollingworth (1988) and Klein et al. (1988)). Both of these factors tend to

produce greater fura-2 saturation. Thus, if the kinetic rate constants for Ca^{2+} binding to fura-2 are underestimated, the magnitude of the error is likely to be larger in skeletal muscle.

Are the data of the present study entirely consistent with fura-2 having rapid Ca^{2+} binding kinetics? It was noted in fura-2 loading experiments, that with increasing fura-2 in the cell, the $[Ca^{2+}]_i$ transient became smaller, as expected, but the time-to-peak $[Ca^{2+}]_i$ was delayed with respect to the furaptra transient and the decaying phase of the transient also appeared to become slower (i.e., Fig. 5 *A* vs. Fig. 5 *B* and Backx and ter Keurs, 1993). As a fast buffer, fura-2 would simply be expected to decrease the size of the transient without affecting its waveform, if there are no other changes in Ca^{2+} release or uptake processes during the transient. A slow buffer, on the other hand, would likely slow the time-to-peak and, possibly, the falling phase of $[Ca^{2+}]_i$ transient with increasing indicator concentration. Thus, although these data could suggest that fura-2 binding kinetics are slow, other explanations for the slowing of the $[Ca^{2+}]_i$ transient are possible. For example, Hollingworth et al. (1992) and Jacquemond et al. (1991) noted that increasing intracellular fura-2 concentration increased SR Ca^{2+} release, presumedly by buffering $[Ca^{2+}]_i$ and thereby decreasing Ca^{2+}-dependent inactivation of SR Ca^{2+} release (Simon et al., 1991). Similarly, in cardiac cells, buffering concentrations of fura-2 in the cell might decrease any Ca^{2+} dependent inactivation mechanism for SR Ca^{2+} release (Fabiato, 1985). This could result in a prolongation of release and, possibly, a delay in the time-to-peak $[Ca^{2+}]_i$. Another possible explanation is that increased buffering by fura-2 decreases $[Ca^{2+}]_i$ which could slow the rate of Ca^{2+} removal from the cytosol. First, Na/Ca exchange rate has been shown to be allosterically regulated by $[Ca^{2+}]_i$ (Miura and Kimura, 1989). Although, this regulation was originally reported to saturate at or below 50 nM $[Ca^{2+}]_i$, other reports (Collins et al., 1992) suggest that concentrations of Ca^{2+} which allosterically regulate transport rate may be much higher. Thus, higher $[Ca^{2+}]_i$ in the furaptra transient may activate faster Na/Ca exchange and increase the decay rate of the transient. Previous data have shown that larger $[Ca^{2+}]_i$ transients decline at a faster rate, independent of the Na/Ca exchange mechanism (Berlin et al., 1990), also consistent with the faster decline of the furaptra Ca^{2+} transient.

In terms of explaining the difference between the amplitude of the $[Ca^{2+}]_i$ transient reported by fura-2 and furaptra, the kinetics of Ca^{2+} binding to fura-2 appear to be rapid enough that the peak $[Ca^{2+}]_i$ will not be significantly increased by correcting for the kinetic limitations of the indicator.

Changes of Ca^{2+}-dependent optical properties of the Ca^{2+} indicators

The optical properties of fura-2 and other fluorescent indicators have been shown to be altered by solution viscosity, pH, ionic strength and presence of proteins (Konishi et al., 1988; Roe et al., 1990; Uto et al., 1991). The sensitivity of indicator fluorescence to environmental factors is a major factor in questioning the accuracy of $[Ca^{2+}]_i$ calculated from indicator fluorescence with the calibration parameters determined in vitro with saline solutions. Li et al. (1987) and the present results demonstrate that the optical properties of fura-2 (as judged by the values of R_{min}, R_{max}, and β) are different in salt solutions and in the myocyte interior. With respect to comparing $[Ca^{2+}]_i$ transients measured by fura-2 and furaptra, this change of calibration parameters is particularly important because only fura-2 calibration requires R_{min}, R_{max}, and β. Using parameters determined in the cell, changes in fura-2 fluorescence convert to $[Ca^{2+}]_i$ transients which are 50–100% larger than when fluorescence is converted to $[Ca^{2+}]$ with calibration parameters determined in salt solutions. Thus, use of in vitro calibration parameters leads to an underestimate of the amplitude of the $[Ca^{2+}]_i$ transient determined from fura-2 fluorescence.

We did not systematically investigate how the K_D for Ca^{2+} of fura-2 and furaptra changes in the cell. However, the Ca^{2+} affinity of fura-2 is reported to decrease in the presence of proteins found in the intracellular environment (Konishi et al., 1988; Uto et al., 1991). Hove-Madsen and Bers (1992) also found that indo-1 bound to cardiac tissue homogenates has a lower affinity for Ca^{2+}. Thus, while the affinity of fura-2 in the myoplasm is unknown, it could be lower than determined with in vitro salt solutions. This conjecture, however, is in contrast to the lack of a marked difference in Ca^{2+} affinity of fura-2 determined in vitro and in iontophoretically loaded papillary muscles (Backx and ter Keurs, 1993) by a calibration technique similar to that used to determine in situ calibration parameters in Fig. 6. The explanation for why Backx and ter Keurs (1993) observe much smaller changes in fura-2 optical properties than the present results and those of Li et al. (1987) and the lack of change in fura-2 Ca^{2+} affinity is not clear.

Fura-2 is approximately 70% bound to cellular constituents in skeletal muscle fibers (Konishi et al., 1988) and cardiac myocytes (Blatter and Wier, 1990). Binding to cellular constituents is also likely to be largely responsible for any change in Ca^{2+} affinity of fura-2 in the cell. Similarly, furaptra is 40–50% bound in skeletal muscle (Konishi et al., 1991), and it seems reasonable to expect that binding of furaptra to cellular constituents would have similar effects on its Ca^{2+} affinity because the indicators are structurally similar (Raju et al., 1989). This idea is supported by preliminary experiments (Mapp and Berlin, unpublished data) which demonstrated that the Ca^{2+} affinity of furaptra was decreased in the presence of proteins, similar to the change in Ca^{2+} affinity of fura-2 (Konishi et al., 1988; Uto et al., 1991). Thus, the absolute Ca^{2+} affinities of fura-2 and furaptra in myocytes are unknown. However, if a shift in Ca^{2+} affinity occurs, it will likely be qualitatively similar for both indicators and will not affect the interpretation of the present results.

CONCLUSION

The size of $[Ca^{2+}]_i$ transients estimated in fura-2-loaded myocytes are smaller than those in furaptra-loaded myocytes under identical experimental conditions. The difference in the size of the $[Ca^{2+}]_i$ transients reported by these two indicators is due to at least two factors, Ca^{2+} buffering by fura-2 and conversion of indicator fluorescence to $[Ca^{2+}]$ with in vitro calibration parameters. Additional factors can not be excluded; however, the Ca^{2+} binding kinetics of fura-2 do not appear to significantly contribute to the smaller size of the $[Ca^{2+}]_i$ transients measured with fura-2. An additional point is that Ca^{2+} buffering by fura-2 may significantly change the time course of the $[Ca^{2+}]_i$ transient even though it appears to behave as a fast Ca^{2+} buffer.

The Ca^{2+} binding kinetics appear to be more rapid than previously reported in skeletal muscle fibers, but the reason why the kinetics would be faster in cardiac myocytes is not clear. These kinetics are rapid enough that fura-2 fluorescence might significantly lag only during the most rapid rise of $[Ca^{2+}]_i$ during a stimulated transient.

These results are also generally applicable because Ca^{2+} buffering by Ca^{2+} indicators and use of in vitro calibration parameters can lead to underestimates of changes in $[Ca^{2+}]_i$ in a variety of cell types.

TABLE 2 Intracellular Ca^{2+} buffers

Species	[ ] (μmol/l)	K_D (M)	k_f (M^{-1} s^{-1})	k_r (s^{-1})
Cellular Ca^{2+} buffers				
Fura-2	84	2.40e-07	2.70e08	65
Troponin-Ca	70	2.00e-06	1.25e08	250
SR Ext. site	47	1.00e-06	1.25e08	125
Sarcolemma	1124	1.00e-04	1.25e08	12500
Cellular Ca^{2+}/Mg^{2+} buffers				
Furaptra -Ca	480	4.70e-05	1.25e08	5875
-Mg		3.60e-03	3.33e04	120
Troponin-Ca	2 × 70	3.30e-09	1.00e08	0.33
-Mg		3.30e-05	3.33e04	1.11
Myosin -Ca	2 × 70	3.33e-08	1.37e07	0.46
-Mg		3.64e-04	1.57e04	0.057
CaMod 1-Ca	6	1.88e-06	1.25e08	235
-Mg		1.96e-03	3.33e04	64.7
CaMod 2-Ca		1.84e-06		230
-Mg		2.92e-03		96.4
CaMod 3-Ca		7.49e-06		938
-Mg		1.25e-03		51.3
CaMod 4-Ca		6.14e-05		7675
-Mg		6.14e-03		203

Intrinsic buffer concentrations and the K_D values are taken from Fabiato (1983). Forward rate constants (k_f) for Ca^{2+} (Robertson et al., 1981) and Mg^{2+} (Konishi and Berlin, 1993) were used to calculate the reverse rate constants (k_r). The forward rate constant for fura-2 was calculated assuming $k_r = 65\ s^{-1}$ (see Appendix II) and $K_D = 239$ nM. Cellular fura-2 concentration was determined in two cells (see Appendix I) and furaptra concentration was assumed to be concentrated in the cell to the same degree as fura-2.

APPENDIX

This appendix describes computer simulations to predict the effects of three potential problems of high affinity Ca^{2+} indicators: 1) Ca^{2+} buffering, 2) kinetic limitations of Ca^{2+} binding, and 3) spatial gradients of $[Ca^{2+}]_i$ within a sarcomere.

I. Ca^{2+} buffering by fura-2

In spite of the results of the experiments described above, we were concerned by the apparently contradictory results reported by Cleeman and Morad (1991). Thus, to examine the question of fura-2 buffering of Ca^{2+}, we constructed a simple computer simulation to predict how many moles of Ca^{2+} might be involved in producing the $[Ca^{2+}]_i$ transients reported by fura-2 and furaptra. The goal of these simulations was to determine if the amount of the Ca^{2+} involved in the transients was similar despite the difference in the size of the $[Ca^{2+}]_i$ transient. This would demonstrate that Ca^{2+} buffering by fura-2 could significantly decrease the amplitude of the $[Ca^{2+}]_i$ transient.

The simulations were very similar to those outlined in Konishi and Berlin (1993) that examined changes in $[Mg^{2+}]_i$ during the $[Ca^{2+}]_i$ transient. In brief, the model used for the simulations assumed the cytosolic space accessible to the indicator and other Ca^{2+} buffers was a single compartment. The total Ca^{2+} involved in the $[Ca^{2+}]_i$ transient ($[Ca^{2+}]_{tot}$) was calculated as the sum of free Ca^{2+} and the concentration of Ca^{2+}-bound intrinsic buffers (CaB_x) at time, t,

$$[Ca^{2+}]_{tot}(t) = [Ca^{2+}]_i(t) + \Sigma CaB_x(t) \quad \text{(A1)}$$

The intrinsic Ca^{2+} buffers are listed in Table 2. The cellular concentrations (expressed as μmol/liter cell H_2O) are taken from Fabiato (1983). These concentrations appear to be reasonable based on the report of Sipido and Wier (1991) who examined intrinsic Ca^{2+} buffering in guinea pig myocytes.

For these simulations, fura-2 would be a major Ca^{2+} buffer so the cellular concentration of fura-2 was examined experimentally by a method similar to that reported by Klein et al. (1988). Briefly, cells with simple rod-shaped geometry were chosen for these experiments and width, length, and depth were measured as described in the Methods section. The cells were voltage-clamped with electrodes containing 50 μM fura-2 and fluorescence during illumination with 360-nm light (i.e., at the isosbestic point) was monitored until near steady-state levels were attained. Fluorescence was then expressed on a per volume basis with the assumption that 25% of cell volume was inaccessible to the indicator. Immediately after the experiment, a glass capillary (10–20 μm diameter) filled with the same fura-2 containing intracellular solution was illuminated with 360-nm light and the fluorescence was adjusted for the illuminated volume of the capillary. Intracellular fura-2 concentration was then calculated by comparing the relative volume-adjusted fluorescence intensities measured in the cell and in the capillary. This procedure was successfully completed in two cells and the intracellular concentrations of fura-2 were calculated to be 82 and 86 μM. Thus, at steady state loading in both cells, fura-2 was concentrated in the cytosol relative to the electrode. This result is not surprising in light of the recent reports showing that fura-2 is highly bound within the myoplasm of skeletal muscle fibers (Konishi et al., 1988) and cardiac myocytes (Blatter and Wier, 1990).

For computer simulations, intracellular fura-2 concentration was assumed to be 84 μM (see Table 2). Similar experiments were not performed to determine the cellular concentration of furaptra, because it was assumed that this indicator would likely be a relatively minor Ca^{2+} buffer within the cell. This assumption was confirmed by the simulations. Nonetheless, furaptra has also been shown to bind to intracellular constituents in skeletal muscle fibers, although to a slightly lesser degree than fura-2 (Konishi et al., 1991). For these simulations, the relative increase in furaptra concentration in the cell was assumed to be the same as for fura-2. Thus, with a pipette concentration of 300 μM in all experiments, the cellular furaptra concentration was assumed to be 480 μM.

$[Ca^{2+}]_{tot}$ was calculated as a function of time by assuming that $[Ca^{2+}]_i$ was initially in equilibrium with all cellular buffers. The change in bound Ca^{2+} to each buffer was calculated using an Euler's numerical integration

routine (Simon, 1972) to solve the following:

$$\frac{dCaB_x(t)}{dt} = B_x(t) \times Ca(t) \times k_{f,x} + CaB_x(t) \times k_{r,x} \quad (A2)$$

where $B_x(t)$ and $CaB_x(t)$ are the free and Ca^{2+}-bound forms of a buffer, respectively. Backward rate constants ($k_{r,x}$) for each intrinsic buffer were calculated assuming the on rate constant ($k_{f,x}$) was 1.25 e08 M^{-1} s^{-1} (Robertson et al., 1981). The intrinsic cellular Ca^{2+} buffers are listed in Table 2. Although there are slow Ca^{2+} buffers within the cardiac cell, particularly the Ca^{2+}/Mg^{2+} sites of troponin C and myosin, our previous simulations of Ca^{2+}/Mg^{2+} competition within the cardiac cell demonstrated that, during the rapid changes in $[Ca^{2+}]_i$, there are only small changes in amount of Ca^{2+} bound to these slow buffers (Konishi and Berlin, 1993). Thus, for the present simulations, these slow buffers have been ignored. Changes in $[Mg^{2+}]_i$ are assumed to be negligible (Konishi and Berlin, 1993). The forward rate constant for fura-2 was calculated by assuming the reverse rate constant was $65s^{-1}$ (Table 2; see Appendix II).

Fig. 7 shows the results of the simulations which compare the estimated amount of Ca^{2+} ($[Ca^{2+}]_{tot}$) involved in the $[Ca^{2+}]_i$ transients measured in myocytes loaded with fura-2 and furaptra. Fig. 7 *A* shows a typical $[Ca^{2+}]_i$ transient in a cell voltage-clamped with an electrode containing 50 μM fura-2 and depolarized from −70 to +10 mV for 50 ms. Resting $[Ca^{2+}]_i$ in this cell was calibrated to be 62 nM, and the peak $[Ca^{2+}]_i$ during the transient was 483 nM. At rest, the total amount of Ca^{2+} calculated to be in the cytoplasm was 15 μmol/liter cell H_2O. During the transient, the waveform of the $[Ca^{2+}]_{tot}$ closely follows that of the $[Ca^{2+}]_i$ transient. This reflects the relatively rapid kinetics assigned to fura-2 and the intrinsic Ca^{2+} buffers. At the peak of the $[Ca^{2+}]_i$ transient, $[Ca^{2+}]_{tot}$ was calculated to be 73 μmol/liter cell H_2O or a change of 58 μmol/liter. In seven cells, the peak change in $[Ca^{2+}]_{tot}$ during the $[Ca^{2+}]_i$ transient averaged 58 ± 8 μmol/liter (Table 1).

For comparison, Fig. 7 *B* shows the result of a simulation carried out for a typical $[Ca^{2+}]_i$ transient from a cell loaded with furaptra. The peak change in $[Ca^{2+}]_i$ was calibrated to be 1.65 μM. The predicted $[Ca^{2+}]_{tot}$ for this transient was 82 μM. The average change in $[Ca^{2+}]_{tot}$ of the furaptra transients listed in Table 1 was 77 ± 9 μM. This value is larger than that predicted for the fura-2 transients, but only by 33%, despite the 4-fold difference in the amplitude of the $[Ca^{2+}]_i$ transients.

Why is it that the 4-fold higher $[Ca^{2+}]_i$ observed in furaptra-loaded cells only translates into a third more $[Ca^{2+}]_{tot}$? The simulations predict that, unlike fura-2, furaptra only binds a small fraction of $[Ca^{2+}]_{tot}$, in spite of the higher furaptra concentration in the cells. The great majority of Ca^{2+}, in the presence of furaptra, is predicted to be bound to the intrinsic Ca^{2+} buffers, particularly troponin C and the sarcoplasmic reticulum Ca^{2+} ATPase. On the other hand, in fura-2-loaded cells, the Ca^{2+} indicator is predicted to be a major buffer, binding similar, if not greater, amounts of Ca^{2+} than troponin or the sarcoplasmic reticulum Ca^{2+} ATPase. Thus, these simulations predict that fura-2 is a potent Ca^{2+} buffer in the myoplasm, consistent with the experimental results.

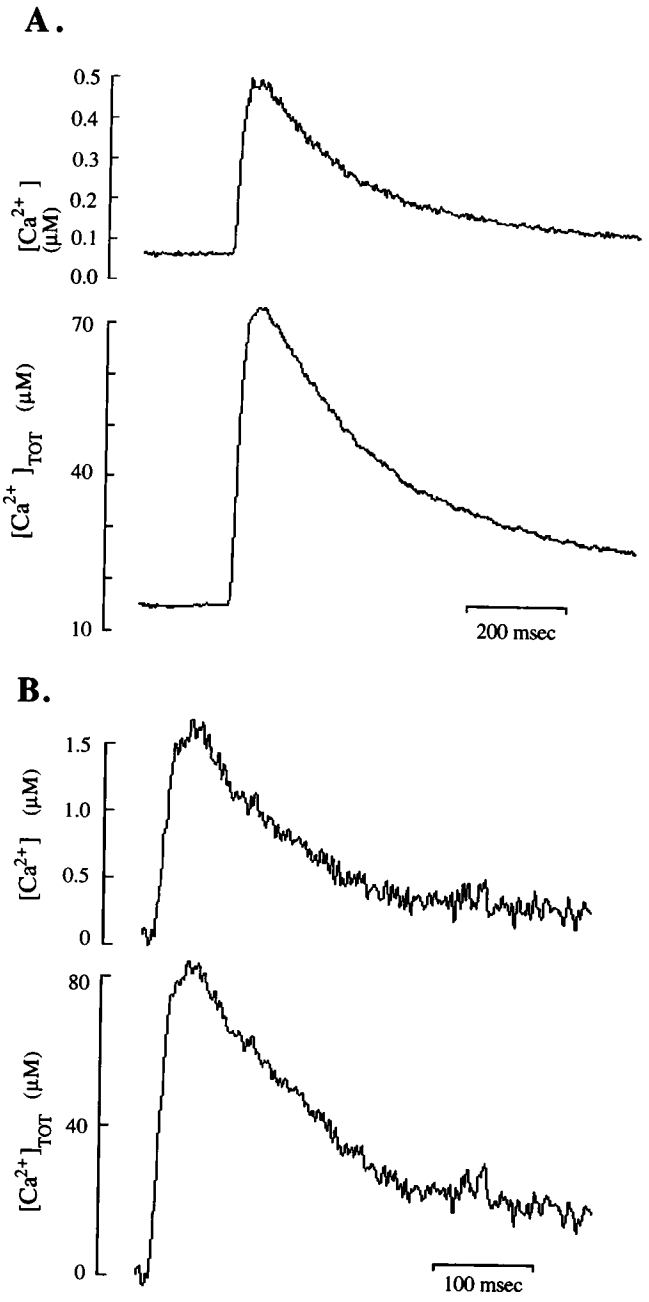

FIGURE 7 Estimation of the moles of Ca^{2+} involved in $[Ca^{2+}]_i$ transients. The top panel is a $[Ca^{2+}]_i$ transient determined in a cell loaded with fura-2 (*A*) and furaptra (*B*). The bottom panel is an estimation of the total $[Ca^{2+}]$ participating in the $[Ca^{2+}]_i$ transient shown in the top panel. Total $[Ca^{2+}]$ (in μmol/liter cytoplasmic H_2O) was calculated with a one-compartment model (see text for details) which included the Ca^{2+} buffers listed in Table 2.

II. Effect of correcting for Ca^{2+} binding kinetics on the calculated $[Ca^{2+}]_i$ transient

Fig. 5 *A* demonstrates that the time course of the $[Ca^{2+}]_i$ transient measured with fura-2 does not show a significant temporal lag when compared to the $[Ca^{2+}]_i$ transient measured in furaptra-loaded myocytes. This indicates that Ca^{2+} binding kinetics do not significantly limit the ability of fura-2 to measure the peak of the $[Ca^{2+}]_i$ transient.

Fig. 5 *B* shows that, with higher intracellular fura-2 concentrations, the peak of the $[Ca^{2+}]_i$ transient did lag behind that of furaptra-loaded myocytes. Although this result is interpreted as an effect of increased fura-2 concentration on cellular Ca^{2+} metabolism (see Discussion), an alternative interpretation (independent of Fig. 5 *A*) is that the lag of the $[Ca^{2+}]_i$ transient in fura-2-loaded cells is due to the kinetics of Ca^{2+} binding to the indicator. To determine what Ca^{2+} binding kinetics would be consistent with this possible interpretation, we attempted to kinetically correct the $[Ca^{2+}]_i$ transient measured with fura-2 to that measured with furaptra. This was accomplished by a graphical procedure similar to that outlined by Klein et al. (1988) which assumes that low affinity Ca^{2+} indicators, such as furaptra, do not have a significant lag in responding to changes in $[Ca^{2+}]$. The fluorescence signal from a high affinity indicator is then mathematically corrected with arbitrarily chosen Ca^{2+} binding rate constants to match the time course of the Ca^{2+} transient measured with the low affinity indicator.

In Figs. 2–7, fura-2 fluorescence has been converted to $[Ca^{2+}]$ with the ratiometric calibration procedure (Grynkiewicz et al., 1985) that assumes the

indicator is in rapid equilibrium with $[Ca^{2+}]$. An alternative procedure is to convert fluorescence ratio to $[Ca^{2+}]$ without any assumptions about the kinetics of Ca^{2+}/fura-2 binding. The equations for this calibration procedure are derived below.

If equilibrium binding between Ca^{2+} and fura-2 (D) is not assumed, changes in the amount of Ca^{2+}-bound fura-2 (DCa) follow a one-to-one binding equation

$$\frac{d[\mathrm{DCa}]}{dt} = [\mathrm{Ca}] \times [D] \times k_{on} - [\mathrm{DCa}] \times k_{off} \tag{A3}$$

where k_{on} and k_{off} are the forward and backward rate constants for Ca^{2+} binding, respectively. Because the fractional bound fura-2 (f) equals the concentration of bound fura-2 divided by the total fura concentration ($[D_{tot}]$),

$$\frac{df}{dt} = \frac{d[\mathrm{DCa}]}{dt} \times \frac{1}{[D_{tot}]}. \tag{A4}$$

Therefore changing fura-2 concentration to fractional bound fura-2 and substituting Eq. A4 into Eq. A3 yields,

$$[Ca^{2+}] = \frac{df/dt + f \times k_{off}}{k_{on} \times (1 - f)}. \tag{A5}$$

To solve the relationship between fluorescence ratio (R) and f, the equation for R from Grynkiewicz et al. (1985) is expressed on terms of f,

$$R = \frac{\alpha_{1F}[\mathrm{D}] + \alpha_{1B}[\mathrm{DCa}]}{\alpha_{2F}[\mathrm{D}] + \alpha_{2B}[\mathrm{DCa}]} = \frac{\alpha_{1F}(1 - f) + \alpha_{1B} f}{\alpha_{2F}(1 - f) + \alpha_{2B} f} \tag{A6}$$

where α_{1F}, α_{1B} are the molar fluorescent coefficients of the indicator at illumination wavelength 1 (340 nm), and α_{2F}, α_{2B} are the coefficients at illumination wavelength 2 (380 nm) for the free and Ca^{2+}-bound forms of fura-2, respectively. Solving for f,

$$f = \frac{(R - R_{min}) \times \beta}{(R_{max} - R) + (R - R_{min}) \times \beta} \tag{A7}$$

where R_{min}, R_{max}, and β have there usual meaning (Grynkiewicz et al., 1985). Substituting Eq. A7 and its derivative into Eq. A5 gives the final equation,

$$[Ca^{2+}] = \frac{\left[\dfrac{dR/dt \times \beta \times (R_{max} - R_{min})}{(R_{max} - R) + (R - R_{min}) \times \beta}\right]}{k_{on}(R_{max} - R)} + \frac{k_{off} \times \beta \times (R - R_{min})}{k_{on}(R_{max} - R)} \tag{A8}$$

The second term on the right-hand side of this equation is the equilibrium solution for R vs. $[Ca^{2+}]$ given in Grynkiewicz et al. (1985), and the first term is the kinetic correction term which depends on the rate of change of fluorescence ratio (dR/dt), k_{on} and experimentally determined constants. Thus, when R is constant, Eq. A8 simplifies to the equilibrium solution. Formally, Eq. A8 is similar to equations derived by Klein et al. (1988) and Sipido and Wier (1991).

This calculation does require discrete values for the forward (k_{on}) and reverse (k_{off}) rate constants for Ca^{2+} binding to the indicator. These rate constants are chosen to optimize the time course of Ca^{2+} transient measured with fura-2 to that measured with furaptra. In these calculations, the fura-2 $[Ca^{2+}]_i$ transient was kinetically corrected to the furaptra transient shown in Fig. 5 *B*.

Fig. 8 shows the fura-2 transient calculated with Eq. A8 and various reverse rate constants chosen so that the K_D (k_{off}/k_{on}) was 239 nM. The fura-2 $[Ca^{2+}]_i$ transient in each panel is scaled and superimposed onto the furaptra $[Ca^{2+}]_i$ transient. The time course of the raising phase and the peak of the $[Ca^{2+}]_i$ transient measured with fura-2 were matched to those of the transient measured with furaptra to determine which of these arbitrarily chosen rate constants would most accurately reflect the true rate constants. As discussed above, this analysis assumes that the $[Ca^{2+}]_i$ transient recorded with furaptra does not lag behind changes in Ca^{2+}.

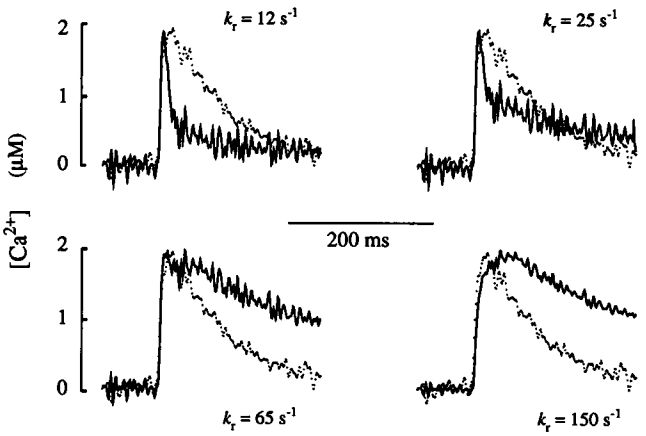

FIGURE 8 Kinetic correction of fura-2 fluorescence signals. Each panel shows the superimposed $[Ca^{2+}]_i$ transients which are the average of those determined in four furaptra (*dashed line*) and three fura-2-loaded myocytes (*solid line*). The fura-2 $[Ca^{2+}]_i$ transients were calculated by converting the ratio of fluorescence intensity (R) to $[Ca^{2+}]$ with Eq. A8 where k_{on} and k_{off} were arbitrarily chosen so that K_D = 239 nM. The reverse rate constant used in the calculation is shown at the top of each panel. The scale factors are 2.0 (k_{off} = 12 s^{-1}), 3.1 (k_{off} = 25s^{-1}), 6.2 (k_{off} = 65 s^{-1}), and 6.4 (k_{off} = 150 s^{-1}). These data are taken from experiments also shown in Fig. 5 *B*.

Changing the rate constants has a profound effect on the shape of the $[Ca^{2+}]_i$ transient calculated from the fura-2 fluorescence transient. With kinetics (k_{off} = 12 or 25 s^{-1}) similar to the reverse rate constants reported by Klein et al. (1988) and Baylor and Hollingworth (1988), a rapid phasic component of the $[Ca^{2+}]_i$ transient is predicted which would not be apparent in the raw fura-2 fluorescence signal. With both these rate constants, however, it is obvious that the predicted rise and fall of $[Ca^{2+}]_i$ occur more rapidly than changes in $[Ca^{2+}]_i$ reported by furaptra. Thus, it is likely that these predicted reverse rate constants for fura-2 are slower than fura-2 kinetics in the myocyte. Conversely, when much faster rate constants are chosen to convert fluorescence ratio to $[Ca^{2+}]$, i.e., k_{off} = 150 s^{-1}, the waveform of the rise in $[Ca^{2+}]_i$ lags behind that measured with furaptra. This suggests that these kinetics are too rapid to be consistent with the observed furaptra fluorescence transient. For the fura-2 $[Ca^{2+}]_i$ transient shown in Fig. 5 *B*, k_{off} = 65 s^{-1} gave the best fit of the rising phase and the peak of the $[Ca^{2+}]_i$ transient determined with furaptra.

By varying k_{off} and k_{on} independently, it was observed that changing k_{off} alters the waveform of the $[Ca^{2+}]_i$ transient predicted from the fluorescence transient, whereas changing k_{on} simply scales the size of the transient without altering its waveform. This is clear when it is considered that k_{off} appears in only one term of Eq. A8, but k_{on} is in the denominator of all terms in the equation.

Only the rising phase and the peak of the fura-2 transient could be fit to the furaptra transient. The inability to fit the entire waveform of the fura-2 transient to the furaptra transient prevented a determination of k_{on} and, therefore, K_D in myocytes. There are two possible reasons for the inability to fit the fura-2 Ca^{2+} transient to the furaptra $[Ca^{2+}]_i$ transient. First, Konishi and Berlin (1993) pointed out that the movement artifact of the furaptra fluorescence signal is as large or larger than the $[Ca^{2+}]$-dependent signal, so that only the rising phase and the peak of the transient can be reliably related to $[Ca^{2+}]_i$. During the declining phase of the transient, which occurs during maximal cell contraction, there is no reliable manner to assure the movement artifact is negligible. Second, the inability to fit the fura-2 transient could be due to fura-2 buffering $[Ca^{2+}]_i$ and the resulting alterations in Ca^{2+} dependent metabolism in the cell (see Discussion).

This calculation, therefore, suggests that the reverse rate constant for Ca^{2+} binding is approximately 65 s^{-1}, a value which is much faster than that calculated in skeletal muscle fibers (Klein et al., 1988; Baylor and Hollingworth, 1988).

III. Influence of intrasarcomere Ca^{2+} gradients on indicator fluorescence signals

To illustrate the effects of dye saturation on the apparent kinetics of indicator binding, we constructed a simple simulation which models the half-sarcomere as a 10-compartment space where each compartment occupies an identical volume (Fig. 9 *A*). Ca^{2+} indicator concentration is equal in all compartments, and Ca^{2+} buffering by the indicator is negligible. Ca^{2+} is released into compartment 1, allowed to diffuse between compartments according to an one-dimensional diffusion equation and is removed from each compartment by a linear process (i.e., far from saturation). In these simulations, Ca^{2+} release occurs for 20 ms at a constant rate. At other times, the release rate is set to zero. During Ca^{2+} release, a steep Ca^{2+} concentration gradient develops from compartment 1 to 10 and then dissipates upon the cessation of release. In this respect, the simulation is qualitatively similar to the half-sarcomere models published by Cannell and Allen (1984) and Wier and Yue (1986).

Fig. 9 *B* illustrates the results of the simulations run where the Ca^{2+} indicator had 1) a K_D of 0.2 μM (similar to fura-2) and 2) a K_D of 20 μM (similar to furaptra). At all times, Ca^{2+} binding to the indicator was assumed to be in rapid equilibrium, i.e., binding kinetics do not influence the results of the simulation. The dotted line shows the $[Ca^{2+}]$ transient reported by the low affinity indicator. This transient peaks at 2 μM and begins to decrease immediately after the cessation of Ca^{2+} release. By comparison, the $[Ca^{2+}]$ transient reported by the high affinity indicator shows a slower rate of raise, a delayed peak and a smaller amplitude (decreased by about 30%). Thus, even in the absence of kinetic considerations, the high affinity indicator reports a smaller transient which appears to be slower than the transient measured with the low affinity indicator. The underlying reason for the different waveforms of the $[Ca^{2+}]$ transient is that the high affinity indicator becomes saturated during the rapid release phase in those compartments with the highest $[Ca^{2+}]$. Thus, the high affinity indicator does not accurately represent spatial mean $[Ca^{2+}]$ under conditions which produce a high degree of indicator saturation. The lag in the fluorescence signal of the high affinity indicator is similar, in some respects, to the kinetic lag of fura-2 reported in skeletal muscle (Baylor and Hollingworth, 1988; Klein et al., 1988).

The graphical method previously used to calculate the kinetic parameters of fura-2 Ca^{2+} binding does not account for the effects of Ca^{2+} gradients within the sarcomere. If these gradients are large (see Cannell and Allen (1984)), it is expected that these calculated parameters will be underestimates of the true Ca^{2+} binding kinetics of fura-2. The magnitude of this underestimate is unknown; however, it could explain the apparent difference between the faster kinetics of fura-2 reported here and those in skeletal muscle (Baylor and Hollingworth, 1988; Klein et al., 1988).

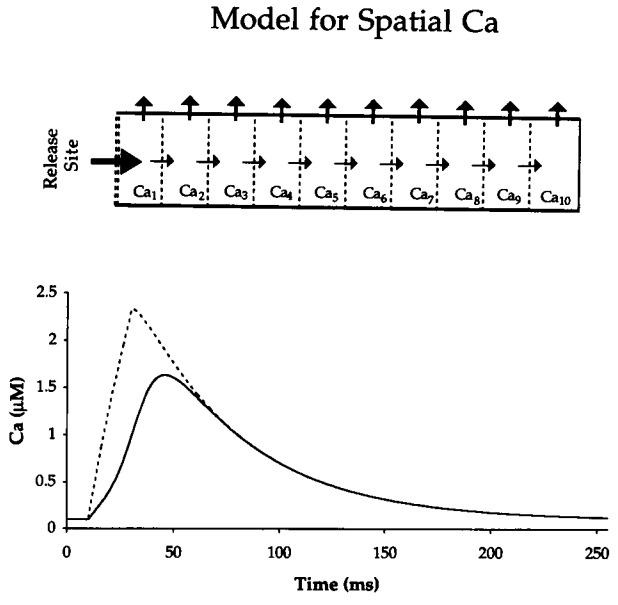

FIGURE 9 Effect of spatial gradients of $[Ca^{2+}]_i$ on the $[Ca^{2+}]_i$ transients measured with a low and high affinity indicator. (*A*) Model half sarcomere. The half sarcomere is modeled as a 10-compartment space where each compartment occupies 0.1 μm^3. Ca^{2+} is released only into compartment 1 but is removed from all compartments (see text for details). (*B*) Ca^{2+} transients estimated with a low (K_D = 20 μM) and high affinity (K_D = 0.2 μM) Ca^{2+} indicator. Superimposed Ca^{2+} transients are calculated by assuming rapid equilibrium between the indicator and Ca^{2+} in each compartment for the high affinity (*solid curve*) and low affinity indicator (*dashed line*). Ca^{2+} release (i.e., input into compartment 1) occurs from 10–30 ms at a constant rate (1.5 μM/ms).

We acknowledge the excellent technical assistance of Anna K. Mapp and the computer programming skills of Alexander J. Fielding. We thank Stephen M. Baylor for helpful discussions.
This work was supported by HL43712 and the Southeastern Pennsylvania affiliate of the American Heart Association (to J. R. Berlin).

REFERENCES

Allen, D. G., and S. Kurihara. 1980. Calcium transients in mammalian ventricular muscle. *Eur. Heart J.* 1:5–15.

Backx, P. H., and H. E. D. J., ter Keurs. 1993. Fluorescent properties of rat cardiac trabeculae microinjected with fura-2 salt. *Am. J. Physiol.* 264: H1098-H1110.

Baylor, S. M., and S. Hollingworth. 1988. Fura-2 calcium transients in frog skeletal muscle fibres. *J. Physiol.(Lond.).* 403:151–192.

Berlin, J. R., and M. Konishi. 1992. Effect of buffering and binding kinetics for fura-2 measurement of transient changes of Ca in cardiac myocytes. *Biophys. J.* 61:A159*a*. (Abstr.)

Berlin, J. R., M. B. Cannell, and W. J. Lederer. 1989. Cellular origins of the transient inward current in cardiac myocytes. *Circ. Res.* 65:115–126.

Berlin, J. R., D. M. Bers, and W. J. Lederer. 1990. Extracellular Na dependent and independent decay of the $[Ca]_i$ transient in rat cardiac myocytes. *Biophys. J.* 57:177*a*. (Abstr.)

Bers, D. M., W. J. Lederer, and J. R. Berlin. 1990. Intracellular Ca transients in rat cardiac myocytes: role of Na-Ca exchange in excitation-contraction coupling. *Am. J. Physiol.* 258:C944-C954.

Blatter, L. A., and W. G. Wier. 1990. Intracellular diffusion, binding and compartmentalization of the fluorescent calcium indicators indo-1 and fura-2. *Biophys. J.* 58:1491–1499.

Blinks J. R., W. G. Wier, P. Hess, and F. G. Prendergast. 1982. Measurement of Ca^{2+} concentrations in living cells. *Prog. Biophys. Mol. Biol.* 40:1–114.

Cannell, M. B., and D. G. Allen. 1984. Model of calcium movements during activation in the sarcomere of frog skeletal muscle. *Biophys. J.* 45:913–925.

Cannell, M. B., and W. J. Lederer. 1986. A novel experimental chamber for single-cell voltage-clamp and patch-clamp applications with low electrical noise and excellent temperature and flow control. *Pflugers Arch.* 406:536–539.

Cannell, M. B., J. R. Berlin, and W. J. Lederer. 1987. Intracellular calcium in cardiac myocytes: calcium transients measured using fluorescence imaging: *In* Cell Calcium and the Control of Membrane Transport. Mandel, L. J. and D. C. Eaton, editors. Society of General Physiologists. Symposium, vol. 42. Rockefeller University Press, New York. 202–214.

Cleeman, L., and M. Morad. 1991. Role of Ca^{2+} channel in cardiac excitation-contraction coupling in the rat: evidence from Ca^{2+} transients and contraction. *J. Physiol. (Lond.).* 432:283–312.

Cobbold, P. H., and P. K. Bourne. 1984. Aequorin measurements of free calcium in single heart cells. *Nature (Lond.).* 312:444–446.

Collins, A., A. V. Somlyo, and D. Hilgemann. 1992. The giant cardiac membrane patch method: stimulation of outward Na^+-Ca^{2+} exchange current by MgATP. *J. Physiol. (Lond.).* 454:27–57.

Fabiato, A. 1983. Calcium-induced release of calcium from the cardiac sarcoplasmic reticulum. *Am. J. Physiol.* 245:C1-C14.

Fabiato, A. 1985. Time and calcium dependence of activation and inacti-

vation of calcium-induced release of calcium from the sarcoplasmic reticulum of a skinned canine cardiac Purkinje cell. *J. Gen. Physiol.* 85: 247–289.

Fabiato, A., and A. Fabiato. 1979. Calculator programs for computing the composition of the solutions containing multiple metals and ligands used for experiments in skinned muscle cells. *J. Physiol. (Paris).* 75:463–505.

Grynkiewicz, G., M. Poenie, and R. Y. Tsien. 1985. A new generation of Ca^{2+} indicators with greatly improved fluorescence properties. *J. Biol. Chem.* 260:3440–3450.

Hamill, O. P., A. Marty, E. Neher, B. Sakmann, and F. J. Sigworth. 1981. Improved patch-clamp techniques for high-resolution recording from cells and cell-free membrane patches. *Pflugers Arch.* 391:85–100.

Harrison, S. M., and D. M. Bers. 1987. The effect of temperature and ionic strength on the apparent Ca-affinity of EGTA and the analogous Ca-chelators BAPTA and dibromo BAPTA. *Biochim. Biophys. Acta.* 925: 133–143.

Hirota, A., W. K. Chandler, P. L. Southwick, and A. S. Waggoner. 1989. Calcium signals recorded from two new purpurate indicators inside frog cut twitch fibers. *J. Gen. Physiol.* 94:597–631.

Hollingworth, S., A. B. Harkins, N. Kurebayashi, M. Konishi, and S. M. Baylor. 1992. Excitation-contraction coupling in intact frog skeletal muscle fibers injected with mmolar concentrations of fura-2. *Biophys. J.* 63:224–234.

Hove-Madsen, L., and D. M. Bers. 1992. Indo-1 binding to protein in permeabilized ventricular myocytes alters its spectral Ca binding properties. *Biophys. J.* 63:89–97.

Inaguma, Y., N. Kurobe, H. Shinohara, and K. Kato. 1991. Sensitive immunoassay for rat parvalbumin: tissue distribution and developmental changes. *Biochim. Biophys. Acta.* 1075:68–74.

Jackson, A. P., M. P. Timmerman, C. R. Bagshaw, and C. C. Ashley. 1987. The kinetics of calcium binding to fura-2 and indo-1. *FEBS Lett.* 216: 35–39.

Jacquemond, V., L. Csernoch, M. G. Klein, and M. F. Schneider. 1991. Voltage-gated and calcium-gated calcium release during depolarization of skeletal muscle fibers. *Biophys. J.* 60:867–873.

Kao, J. P. Y., and R. Y. Tsien. 1988. Ca^{2+} binding kinetics of Fura-2 and Azo-1 from temperature-jump relaxation measurements. *Biophys. J.* 53: 635–639.

Klein, M. G., B. J. Simon, G. Szucs, and M. F. Schneider. 1988. Simultaneous recording of calcium transients in skeletal muscle using high and low affinity calcium indicators. *Biophys. J.* 53:971–988.

Konishi, M., and J. R. Berlin. 1991. $[Ca^{2+}]_i$ transients in cardiac myocytes measured with high and low affinity calcium fluorescent indicators. *Biophys. J.* 59:542*a*. (Abstr.)

Konishi, M., and J. R. Berlin. 1993. Ca transients in cardiac myocytes measured with a low affinity fluorescent indicator, furaptra. *Biophys. J.* 64:1331–1343.

Konishi, M., A. Olson, S. Hollingworth, and S. M. Baylor. 1988. Myoplasmic binding of fura-2 investigated by steady-state fluorescence and absorbance measurements. *Biophys. J.* 54:1089–1104.

Konishi, M., S. Hollingworth, A. B. Harkins, and S. M. Baylor. 1991. Myoplasmic calcium transients in intact frog skeletal muscle fibers monitored with the fluorescence indicator furaptra. *J. Gen. Physiol.* 97:271–301.

Li, Q., R. A. Altschuld, and B. T. Stokes. 1987. Quantitation of intracellular free calcium in single adult cardiomyocytes by fura-2 fluorescence microscopy: calibration of fura-2 ratios. *Biochem. Biophys. Res. Commun.* 147:120–126.

Marban, E., M. Kitakaze, Y. Koretsune, D. T. Yue, V. P. Chacho, and M. M. Pike. 1990. Quantification of $[Ca^{2+}]_i$ in perfused hearts. *Circ. Res.* 66: 1255–1267.

Martell, A. E., and R. M. Smith. 1974. Critical Stability Constants. Vol. 1: Amino Acids. Plenum Publishing Corp., New York. 199–269.

Maylie, J., M. Irving, N. L. Sizto, and W. K. Chandler 1987a. Calcium signals recorded from cut twitch fibers containing Antipyrylazo III. *J. Gen. Physiol.* 89:83–144.

Maylie, J., M. Irving, N. L. Sizto, G. Boyarsky, and W. K. Chandler 1987b. Calcium signals recorded from cut frog twitch fibers containing tetramethylmurexide. *J. Gen. Physiol.* 89:145–176.

Miura, Y., and J. Kimura. 1989. Sodium-calcium exchange current dependence on internal Ca and Na and competitive binding of external Na and Ca. *J. Gen. Physiol.* 93:1129–1145.

Raju, B., E. Murphy, L. A. Levy, and R. E. London. 1989. A fluorescent indicator for measuring cytosolic free magnesium. *Am. J. Physiol.* 256: C540-C548.

Robertson, S. P., J. D. Johnson, and J. D. Potter. 1981. The time-course of Ca^{2+} exchange with calmodulin, troponin, parvalbumin, and myosin in response to transient changes in Ca^{2+}. *Biophys. J.* 34:559–569.

Roe, M. W., J. J. LeMasters, and B. Herman. 1990. Assessment of fura-2 for measurements of cytosolic free calcium. *Cell Calcium.* 11:63–73.

Simon, W. 1972. Mathematical Techniques for Physiology and Medicine. Academic Press, New York. 267 pp.

Simon, B. J., M. G. Klein, and M. F. Schneider. 1985. Calcium dependence of inactivation of calcium release from the sarcoplasmic reticulum in skeletal muscle fibers. *J. Gen. Physiol.* 97:437–471.

Sipido, K., and W. G. Wier. 1991. Flux of Ca^{2+} across the sarcoplasmic reticulum of guinea-pig cardiac cells during excitation-contraction coupling. *J. Physiol.(Lond.)* 435:605–630.

Timmerman, M. P., and C. C. Ashley. 1986. Fura-2 diffusion and its use as an indicator or transient free calcium changes in single striated muscle cells. *FEBS Lett.* 209:1–8.

Uto, A., H. Arai, and Y. Ogawa. 1991. Reassessment of fura-2 and the ratio method for determination of intracellular Ca^{2+} concentrations. *Cell Calcium.* 12:29–37.

Wier, W. G., and D. T. Yue. 1986. Intracellular calcium transients underlying the short-term force-interval relationship in ferret ventricular myocardium. *J. Physiol. (Lond.)* 376:507–530.